

Please find our comments (non-italicized) to the Reviewer #1 (italics) addressed below:

Overall this paper is interesting but not entirely convincing. However, it is the authors staking their reputation on this and I will not stand in their way. However, I hope that the many co-authors are sufficiently convinced that they will not also agree to be coauthors any paper using their data that comes to a different conclusion about high NO_x photochemistry. There are three major issues the authors should address:

We thank the reviewer for his or her time spent on providing a review for this manuscript. We agree that the results presented here are not entirely convincing and have conducted further laboratory tests, improved our data analysis, done more model runs, and re-written the manuscript to focus on the evidence for ozone production rates and its implications.

We will ignore the reviewer's second sentence – perhaps the reviewer should be gently reprimanded by the editor for it? The third sentence is interesting in that it implies that doing science is staking a position and sticking to it, even if previous evidence is found to be wrong or is overwhelmed by the weight of new evidence. In our view, science advances as evidence accumulates and scientists should change their thinking in light of new evidence, even if it contradicts their previous conclusions. So we respectfully disagree with the reviewer on these two sentences.

On the other hand, the reviewer makes many good points in the rest of the review and we will do our best to answer them.

1) They dismiss large negative values but not large positive values as unphysical. It is not clear that both types of errors shouldn't be treated as representative of the random error of the method used.

As pointed out in Baier et al. (2015), this technique seems to produce a large negative differential ozone signal that is roughly correlated with temperature, relative humidity, or actinic flux. This negative ozone differential is not related to negative chemical ozone production because it occurs even when the reference chamber film has been removed from the reference chamber (so that ozone production is the same in both chambers) and on low ozone production days with low levels of actinic flux and precursor gases. It should be noted that the raw P(O₃) data show positive deviations from this negative pattern between 0800-1200 LT on most days. Thus, this large negative is related to something occurring in the chambers or in the Thermo ozone monitor.

After we received the reviews, we investigated in the laboratory that sensitivity of the Thermo 49C ozone monitor to relative humidity and to temperature. We did not find a strong correlation between differences in temperature between the sample and the reference chamber, but we did find a rather large shift in the Thermo instrument zero as a function of relative humidity equivalent to roughly 70% ambient relative humidity. The shift is almost binary, with an offset that is steady up to within a few percent of a certain relative humidity and then a sudden shift of ~2 ppbv within a few percent around that value. Thus, we restrict our analysis to days with lower relative humidity, when we are confident that a relative humidity initiated ozone offset change did not happen.

Four zeros were applied to the raw P(O₃) data during the campaign. Two were by removing the ultem (reference chamber) film for an entire 24-hour period and two were using known low ozone production days as zeros. To avoid the problems with the sudden shift in the instrument zero, we have restricted our analysis to days when the ambient relative humidity was below 70%. In addition, we use zeros only from days that have similar relative humidity values and variations as the days for which the ozone production rate is being measured.

We include a figure of the resulting $P(O_3)$ offset that we subtracted from the observed $P(O_3)$ measurement in the Supplemental Information Figure S1 in order to get the corrected $P(O_3)$ that is shown in subsequent figures within the manuscript.

In order to ensure that the reported $P(O_3)$ values were not sensitive to our choices, we varied the threshold relative humidity and the choice of zero days that we used in the analysis over wide ranges. While the peak ozone production rate varied from 8 to 15 ppbv/hr and the minimum early evening values varied from 2 to -4 ppbv/hr, the overall shape of the measured ozone production rate was the same (i.e. MOPS corrected $P(O_3)$ data increase around 0800 LT, peak around 9-11 LT, and then decrease later in the day. We added a figure in the supplemental material to show this (Figure S2).

We used a Thermo 49C instrument to make these measurements, and at the level of the expected ozone difference from chemical ozone production (i.e. an ozone differential of 0.3 ppbv is equivalent to 8 ppbv/hr), the data are noisy and need to be integrated over time to reduce the noise. In Figure 1 that shows the measured values as a function of day of the year, we chose a one-hour average as opposed to the 30-minute averages chosen in the original manuscript submission. It is clear that the negatives are no longer as prominent – mainly because of the improved zero correction and partly because of the increased integration time, but the positive feature at ~1000 LT remains quite robust.

Additional information has been added on Pg. 6 lines 4-22 outlining these comments above, as well as in Section 1 in the Supplemental Information. We have also added the following lines to section 3.2 Pg. 11 lines 6-11:

“Third, when different relative humidity thresholds are used to correct the raw $P(O_3)$ data, measured $P(O_3)$ consistently exhibits the same diurnal behavior with a positive deviation from modeled $P(O_3)$ around 1000 LT. Fourth, deviations from the O_3 differential baseline derived from zeroing methods are observed between 0900-1100 LT even before correcting the MOPS measurements. Thus, we have confidence in the positive MOPS $P(O_3)$ signatures, which are greater than the modeled $P(O_3)$ during the morning hours.”

2) Much is made of the linear NO_x dependence of the model observation mismatch. A figure showing this should be presented.

We should correct ourselves in that the model-data mismatch increases monotonically for increasing NO above 1 ppbv. A figure showing the NO dependence of the model observation mismatch now been added to the manuscript (now Figure 4) along with the following text on page 10 line 31 to page 11 lines 1-2:

“The missing modeled $P(O_3)$ appears to be monotonically increasing with NO for NO values greater than roughly 1 ppbv (Fig. 4). The difference between measured and modeled $P(O_3)$ is near zero up to 1 ppbv NO and almost 15 ppbv/h at 5 ppbv NO. This unexpected increase in $P(O_3)$ with increasing NO provides a clue as to what might be causing the difference between measured and modeled $P(O_3)$.”

3) The authors dismiss HONO and VOCR as a potential source of discrepancies too easily. It would be better to instead assume the entire discrepancy is due to HONO or to VOCR that is correlated with NO and show the reader the relationships between NO, HONO and VOCR that would be required to explain the results. Then the reader can judge whether those ideas are plausible.

This is a good suggestion. We have added to Sections 3.3.3 and 3.3.4, which use model calculations to assess whether HONO or RO_2 sources could potentially explain the model-data mismatch during the morning hours. We have further described the effect that these two additional $P(O_3)$ sources have on

the HO₂/OH ratio as a function of NO, but have not been able to reproduce the measured HO₂/OH NO_x dependence. (Please see the following comments below that discuss the plausibility of HONO as a morning P(O₃) source.)

An additional HO₂ source via the generic reaction RO₂ + NO → HO₂ + NO₂ + R'O was added to the MCMv331 using CH₃O₂ as the organic peroxy radical. However, the addition of this reaction elevates the entire modeled P(O₃) curve throughout the day and does not alter morning P(O₃) patterns relative to the MOPS. Additional RO₂ added to the MCMv331 proportional to approximately 0.05% NO_x was added to the MCMv331, which more closely replicates the MOPS morning P(O₃), but underestimates the MOPS afternoon P(O₃). Please see Figure 6, which was taken from the supplemental material and added to the main text. We have added text beginning on Pg. 13 line 28 to Pg. 14 lines 1-15 to discuss the plausibility of missing model RO₂/VOCR.

Other comments

Page 2 Line 27: Only the formation of peroxyacyl nitrates, and not alkyl nitrates, is a form of Ox loss. The reaction RO₂ + NO → RONO₂ does not produce or consumer either O₃ or NO₂.

Fixed in Eq. 3. Pg. 2 lines 26 – Pg. 3 line 1 now read:

“Equation 3 describes the chemical O₃ (or NO₂) destruction rate or rate of removal to reservoir species as the fraction of O₁D molecules resulting from O₃ photolysis that react with H₂O to form OH; reactions of O₃ with HO_x (HO₂ + OH); the net production of peroxyacyl nitrates (PANs); the reaction of OH and NO₂ to form nitric acid (HNO₃) and O₃ loss through reactions with alkenes and halogens.”

Page 2 Line 27: Equation 3 includes the production of nitric acid via OH + NO₂ - this should also be included in the description of ozone chemical loss processes.

Fixed in Eq. 3 and on Pg. 2 lines 26- Pg. 3 line 1.

Page 4 Line 1- 3: It would be useful to understand which of these references are from ambient field studies and which (if any) are from chamber studies. Some of the proposed explanations of the MOPS v. Modeled PO₃ in this paper should exist in both field and chamber studies (e.g. OH + NO₂ + O₂) while others (e.g. ClNO₂) are unlikely to be a factor in chamber studies.

All of the studies listed in the last paragraph on Pg. 4 lines 5-7 are field studies. To our knowledge, no chamber studies have been published that explain the measured vs. modeled P(O₃) discrepancy or the HO₂/OH vs. NO discrepancy also mentioned. Thus, to our knowledge, there have not been any chamber studies conducted that could propose an explanation to the results shown in this manuscript. The proposed reaction (OH + NO₂ + O₂) has been removed as a possible solution to the observed model-data mismatch.

Page 4 Line 13 - 20: It is unclear what this paragraph is actually describing. Are these results all from a single study, or are these similar results from a variety of MOPS deployments?

We clarify this sentence to state which deployments (and when) were MOPS deployments, and to note that all of the other studies referenced were field studies. Pg. 4 lines 28-30 now read:

“Due to the aforementioned discrepancies between measured and modeled radicals, P(O₃) calculated from measured peroxy radicals can routinely be more than double the P(O₃) calculated from modeled HO₂ or RO₂ at high NO_x according to several field studies conducted during the past decade...”

Page 4 Lines 33-37 now read:

“For example, in 2010 the first version of the MOPS (Cazorla et al., 2012, Ren et al., 2013 compared directly-measured O₃ production rates to both modeled P(O₃) and that calculated from measured peroxy radicals. Observed P(O₃) was approximately equal to that modeled for NO levels up to 1 ppbv, but was significantly larger for higher values of NO.”

Page 8, Line 22: Were time periods selected for removal based on the humidity or of the MOPS measurement itself? It is unclear from the description in this paragraph and should be clarified.

Please read the description of the analysis method given earlier in our responses.

Page 9, Line 17-19: While Figure 1 shows several days where the MOPS peak PO₃ value is between 10-20 ppb/hr greater than the modeled value, it also shows several days where the MOPS minimum PO₃ value is between -10 and -20 ppb/hr (e.g. Jul 21, 23, 24, Aug 6). Since these large negative values are explained as non-physical, why is it not equally plausible that the large positive values are a measurement artifact as well?

Please read the description of the analysis method given earlier in our responses. Many of these large negative deviations have been reconciled with a) averaging to 1-hour time periods and b) through revising the correction of the raw P(O₃) data to account for only days when the relative humidity was less than 70%.

Page 11 Line 12 & Page 12 Line 5: The claim that the difference between MOPS and Modeled PO₃ is linear with NO is difficult to evaluate from the figures provided. Since the NO dependence of the MOPS-Model disagreement is an important part of the analysis, the authors should include a figure that directly shows the difference in PO₃ during the morning as a function of NO.

Please see our comment addressing this above. Figure 4 has been added in the text.

Page 12, Line 8-9: This sentence appears to contradict section 2.2, where median diurnal values of VOCs are said to be used in the model calculation. The authors should clarify how the model includes the dependence of VOC reactivity on NO.

We should clarify that the model includes the average VOC reactivity dependence on NO. VOC reactivity is linked to the median diurnal values of the VOCs used to constrain the model. Thus, the whole-air sampled VOCs are the available sources providing an average dependence of VOC reactivity on NO in the chemical mechanisms used in this study. We have stated this on Pg. 13 lines 24-26:

“Although measurements of VOC reactivity were not available during the field campaign time period and thus are unavailable for comparison to modeled VOC reactivity, the suite of VOCs measured in Golden should sufficiently capture the average VOC reactivity dependence on NO in the mechanisms used here.”

Page 12, Line 15-17: As written, the proposed OH + NO + O₂ -> HO₂ + NO₂ reaction seems to be an OH loss as well as an HO₂ source. The authors should clarify why the argument here against a missing VOC source do not also apply to this proposed reaction.

This proposed reaction has been removed from the analysis, as preliminary laboratory testing and theoretical work has shown that this reaction is highly unlikely. Please see our comment above about a missing VOC source.

Page 12, Line 27-Page 13, Line 5: I am uncertain whether the mechanisms listed in this paragraph are candidates for the OH + NO + O2 reaction mechanism or not. Rewording this paragraph to clarify what some possible forms of this reaction are, and whether it might involve additional species such as acetylene would be useful.

This paragraph has been omitted.

Section 3.3.6: Given the known difficulties models have in capturing HONO concentrations, this section feels overly brief in dismissing HONO as a HOx source. I would appreciate at least brief consideration of what magnitude HONO source would be necessary to make the modeled PO3 values match the MOPS values.

Section 3.3.4 has been thoroughly modified on Pg. 14 starting on line 16. We have conducted additional model tests in order to describe the magnitude of a HONO source that would allow the modeled P(O₃) and MOPS P(O₃) to match. We have also described model sources of ambient HONO here. An additional HONO source is one probable missing element from our model analyses. As HONO production should be linearly dependent upon NO_x levels, additional HONO is added to MCMv331 as 10% of NO_x values, yielding peak HONO levels at 1000 LT of 0.9 ppbv. While the modeled P(O₃) with added HONO best replicates the MOPS diel P(O₃) pattern shown in Figure 6 out of all of the model case studies conducted for this analysis, HONO levels needed to do so are almost twice levels observed at a nearby observation site in Colorado as well as in other, more polluted areas. Modeled peak P(O₃) is shifted to approximately an hour later than the MOPS and is slightly overestimated in the afternoon. We have added the following text on Pg. 15 lines 3-10 to indicate this:

“A HONO source proportional to NO_x was added to the MCMv331, resulting in average HONO levels of 0.5-0.9 ppbv between 0700 and 1200 LT, with peak HONO levels of 0.9 ppbv at 1000 LT when MOPS P(O₃) exhibits its diel peak. This case study approximately replicates the observed morning P(O₃) and observed OH within uncertainty levels (Fig. 6). However, while added HONO in the MCMv331 improves the agreement between observed and modeled diel P(O₃), mid-morning HONO levels needed to do so are over a factor of two higher than those observed in other areas within Colorado (Brown et al., 2013; Vandenboer et al., 2013) and in environments with much higher NO_x levels (Vandenboer et al., 2015). Thus, the HO₂/OH ratio and the abnormally high HONO required to match the observed P(O₃) provide evidence that at most only a part of the observed P(O₃) can be explained by atmospheric HONO.”

Figure 5: If the disagreement between measured and modeled PO3 is strictly a function of NOx, why is the disagreement so much worse on plume days, even though plume and non-plume days both have average morning NO concentrations of approximately 2 ppb? Are there other significant differences between plume and non-plume days, or is there significantly more variability in the amount of NOx on plume than on non-plume days?

The difference between measured and modeled P(O₃) is dependent upon NO_x. We have shown that the chemical mechanisms may be missing a hydroperoxy radical source co-emitted with NO relative to measurements and have explored several model case studies to try to reconcile this model-measurement disagreement.

It is noted in Section 2.2 Pg. 7 lines 27-30 that NO_x and VOCs are both higher, on average, on plume days than on non-plume days. We have also shown that there can be significant differences (~5-10

ppbv/h) between the modeled and MOPS $P(O_3)$ at NO levels greater than approximately 1 ppbv. Thus, the difference between the MOPS and models on plume vs. non-plume days is consistent with this result.

We have added the following text to Pg. 17 lines 10-12:

“Measured O_x maxima are 2-7 ppbv greater on these “plume” days than when air is advected from elsewhere, and higher $P(O_3)$ is measured by the MOPS than is modeled by the RACM2 and MCMv331 (Fig. 7). This result is roughly consistent with the difference between measured and modeled $P(O_3)$ as a function of NO shown in Fig. 4.”

Technical Corrections Page 12, Line 12: If this number is a rate of HO₂ production, then the units on this are incorrect (perhaps intended to be radicals cm⁻³ s⁻¹?)

Corrected.

Page 13, Line 1-2: In this sentence, the phrase “the formation of” appears to be extraneous. The accent on FRAPPÉ is inconsistent. Sometimes the campaign is incorrectly written as FRAPPÈ.

Corrected.

Please find our comments (non-italicized) to the Reviewer #2 (italics) addressed below:

The manuscript describes a comparison of P(O3) measured using a second generation MOPS instrument and P(O3) modelled using a detailed chemistry mechanism (MCMv3.3.1) and lumped chemistry scheme (RACM2). A higher measured than modelled P(O3) is reported during the morning hours and the authors postulate that this discrepancy could be caused by a model under-estimation of HO2 under high NOx conditions and present a possible reaction which cycles OH to HO2 via NO that could rectify the discrepancy. The manuscript concludes with a discussion on how these model uncertainties may influence ozone reduction strategies in the region. From reading this manuscript in detail, I have not been convinced that the differences reported between modelled and measured P(O3) are not, in part, caused by instrumental issues (I have detailed my specific concerns below) and to a smaller extent, caused by uncertainties in the model constraints (e.g. the interpolation of the VOC measurements and the use of a constant, median VOC value for certain VOCs). I cannot recommend publication in ACPD before the specific comments I have raised below are adequately addressed.

We thank the reviewer for presenting several important points to be addressed in the manuscript. We note that we have adjusted the manuscript focus to address peroxy radical (HO₂ and RO₂) discrepancies at high NO_x and have performed additional model case studies exploring the plausibility of missing peroxy radical sources. Since we proposed the reaction OH + NO (+ O₂) to form HO₂ + NO₂ earlier in 2016, preliminary work in our laboratory and that of a colleague, as well as a theoretical study, have all indicated that this reaction is unlikely. We have thus decided to omit this reaction as an explanation to the model-data mismatch described in the main text. We have instead explored the plausibility of missing peroxy radicals and other chemical causes.

Throughout the manuscript, the authors argue that the higher observed P(O3) than modelled P(O3) at high NO is supported by observations of higher (than modelled) HO2 under high NO conditions. Only recently, however, have HO2 measurements been reported in the literature that have not been influenced by artefact signals induced by the fast decomposition (within instruments) of certain RO2 species. The authors do not discuss recent observations and model comparisons made in China (Tan et al., 2017) where interference-free HO2 observations agree well with model predictions under elevated NO conditions. The authors need to provide a more balanced discussion of modelled and measured HO2 comparisons under high NO conditions which includes a review of the possible problems relating to HO2 measurements as well as the more recent HO2 modelled and measured comparisons.

The introduction has been modified to include a) known HO₂ measurement interferences and b) an extended literature review of HO₂ measurement comparisons with models including more recent studies. This extension of the introduction includes a synthesis of comparisons made in high and low-NO environments in various studies (Stone et al. (2012)) as well as other studies such as Tan et al. (2017) and Hofzumahaus et al. (2009), which show small and/or insignificant

model HO₂ underprediction during morning hours. However, Tan et al. (2017) HO₂ measurements do not suffer from the RO₂ interference and yet still exhibits slight underprediction of HO₂ at high NO_x. The highest NO values reported for some of these studies was only a few ppbv as in Tan et al., 2017. For many studies, the separation between measured and modeled HO₂ is within uncertainties at these low NO levels but then grows at higher NO levels, particularly above 10 ppbv. Thus, even when accounting for HO₂ interferences, model underestimation of HO₂ at high NO_x appears to be robust. If the ratio of atmospheric RO₂ to HO₂ is used to predict a maximum HO₂ interference, this interference can be approximately a factor of two higher than HO₂. Thus, an HO₂ interference is not the sole cause for model-data HO₂ mismatch at high NO_x presented in the literature studies outlined in the introduction. These ideas have also been added to Pg. 3 lines 1-25.

We have also modified the introduction to describe model RO₂ underestimation, presenting this as a viable reason for model P(O₃) underprediction. Model peroxy radical underestimation at high NO is therefore outlined throughout the rest of the paper as a possible cause for model underestimation of P(O₃) and case studies are presented in the revised manuscript.

Pg 5, line 8 -16: The authors discuss the influence of humidity on the O3 analyser used in the MOPS instrument and cite previous papers which have reported large changes in O3 concentration as RH is rapidly changed. How fast and by what percentage did RH typically change during these ambient measurements made in Golden? Did the authors attempt to correct for this RH dependence?

Additional laboratory studies have been conducted to address this comment. Please see our comments for Reviewer 1 that address this issue.

Pg 5, line 23: 'some excess HONO was measured..' how much and how did this vary with RH, T, [NO2] and actinic flux? Would this excess HONO be expected to be greatest during the morning hours when NO2 concentrations were high? Details like this need to be provided so the differences reported between modelled and measured P(O3) during the morning hours can be fairly assessed.

We would expect the HONO bias to be greatest during the morning hours when NO_x, relative humidity, and actinic flux is high. However, we would expect that the P(O₃) bias due to excess HONO production in Golden, CO be considerably smaller as we have been able to decrease this bias ~ 30% in State College, PA (Baier et al. 2015) by covering the MOPS inlet face to avoid excess HONO production and photolysis, and as NO_x levels Golden, CO are considerably smaller than in Houston, TX. The relative humidity and NO_x levels in Golden, CO were significantly lower than in Houston, TX, while the actinic flux is similar.

Model calculations of the MOPS HONO bias using the measured chamber HONO to observed NO_x ratio in Houston, TX and scaling this ratio to the observed NO_x in Golden, CO indicate a bias of 3 ppbv/h. However, in this estimation, we did not consider that only a small fraction of chamber-generated HONO would be photolyzed within the residence time in the chamber,

which makes this potential positive P(O₃) interference less than 0.5 ppbv/h and thus insignificant. We expect that, since this bias is considerably smaller than the difference between measured and modeled P(O₃) shown in Figure 1, the model-measurement P(O₃) mismatch is not due to this artifact.

We have added lines Pg. 6 line 32 to Pg. 7 line 5 describing what we have done to decrease the HONO bias. We have added how we have calculated this potential HONO bias for Golden, CO on Pg. 11 line 30 to Pg. 12 line 8.

Pg 5, line 24: ‘..actions were taken’. Some details on the actions that were taken should be provided here.

Please see previous comment.

Pg 6, discussion of model constraints: I have some concerns over how well the model constraints represent the local conditions in Golden. How many WAC samples were collected between 0700 – 1200? I worry that interpolating these canister samples may lead to underestimations in peak VOC concentrations.

A total of 46 whole-air canister samples were taken between 0700-1200 LT. Therefore, over 64% of the WAC samples were taken during the morning hours. As continuous VOC measurements were not available in Golden, CO, it is not possible to determine median diurnal values of these VOCs in any other manner. We have added the following text to lines 18-24 on Pg. 7:

“In the absence of continuous ground-based VOC measurements, C₂-C₁₀ non-methane hydrocarbons (NMHC) and organic nitrates were measured from 72 total whole-air canister (WAC) samples that were collected in Golden and analyzed by gas chromatography (GC) and gas chromatography-mass spectrometry (GC-MS) in the laboratory. An average of five samples were taken daily over 16 days, with approximately 64% of sampling occurring between 0700 and 1200 local time (LT) to capture VOC mixing ratios during morning O₃ production hours, and sparser sampling in the afternoon between 1400 and 1800 LT to examine advection from sources east of Golden, CO such as the Denver metropolitan and Commerce City regions.”

In addition, Shirley et al. (2006) employ a similar approach to estimating VOC abundances, but use OH reactivity measurements to calculate VOC speciation abundances. Given several model sensitivity runs varying these VOCs, we expect that the estimation of VOC abundances in this manuscript can adequately capture diurnal variations -- in an average sense -- in order to compare hourly measured and modeled P(O₃) rates in Figure 2.

In table S1 the authors state that constant, median values of various species measured on board the aircrafts were used to constrain the model. How can this be a valid approach given the high variability of some of these species, e.g. the biogenics? Would this variability bias the model predictions as a function of time of day? I.e. were VOC concentrations highest during the morning when the boundary layer was lowest? It is unclear if the sensitivity

analysis conducted (presented in Fig S1) included varying VOC concentrations by the observed variability or varying by the uncertainty in the VOC measurement only?

Aircraft measurements in the boundary layer for areas surrounding Golden, CO were available after 9am LT for the P-3B and after 10am LT for the C-130. Thus, the concentrations of aircraft VOCs used in this analysis are limited to mainly after 9-10am LT and early morning concentrations were not known. Because of this limited aircraft data, the few morning VOC species that were measured on aircraft are set at constant, median values, while the majority of VOCs are taken directly from whole-air canister samples as described above. For those chemical species measured in common between the aircraft and the ground site, the agreement is within 30% on average. Further, biogenic chemical species do not have a substantial role in OH reactivity in Golden and so would have a smaller impact on modeled $P(O_3)$. Thus, the most important chemical species measurements for ozone production came from the whole air sampler on the ground. We have added Pg. 7 line 33 to Pg. 8 line 5 to clarify the few aircraft points that we have available to incorporate into the model:

“Canister VOCs were supplemented by boundary layer inorganic and organic chemical species measurements obtained on the NASA P-3B and NSF/NCAR C-130 aircraft and constant, median values were calculated for the limited times of the day when these aircraft were in the vicinity of Golden and used in the model (Table 1, Table S1). Aircraft measurements for Golden were available after 0900 LT on P-3B overflights, which occurred up to three times daily, while C-130 measurements were available after 1000 LT when this aircraft was within roughly 20 km of the measurement site. Airborne measurements of inorganic and organic species agree to within 30% on average.”

The analysis in Table S1 is conducted by varying the VOC concentrations by their uncertainty only in order to determine the total model uncertainty that is due to parameter uncertainties as in Chen et al (2010). This analysis was conducted to solely investigate the dependence of model uncertainty on model parameter uncertainties.

Pg 7, line 1: ‘..integrated for 24 hours..’ I would be surprised if the reactive intermediates and, more importantly, modelled HO₂ and RO₂ are in steady state after 24 hours. By what percentage did the modelled peroxy radical concentrations change from day 1 to day 2?

Additional MCMv331 model runs have been conducted that vary the integration time from one to three days with little difference seen between model HO₂, RO₂, or OH for these three different model integration times. Therefore, we do not expect these species to vary significantly whether we use a one-, two-, or three-day integration period for model runs. We have further explained this result on P8 lines 16-18 and deem a 24-hour integration period for these species acceptable:

“In addition, a one-day integration time is calculated to be sufficient for radical concentrations and intermediate species to reach steady-state as a two-fold or even three-fold increase in this

integration time period does not impact radical concentrations or the P(O₃) results described below.”

Pg 8, line 19: How does the diel measured P(O₃) change if the negative P(O₃) points are not omitted? By omitting these negative points, does this not positively bias the P(O₃) measurements in the morning when these negative points are most frequent? Were the modelled P(O₃) calculated at the same time also removed? Could the authors be more quantitative when they discuss the O₃ analyser RH dependence – what do they class as a ‘drastic change’ in RH?

Please see our comments for Reviewer 1 on this issue.

Section 3.2 would benefit from Rate of Production Analysis. This would help to reveal what is driving the high modelled P(O₃) on certain days. It would also reveal the cause of the differences that were observed between RACM and MCM at times rather than rely on speculation ‘..perhaps due to more explicit treatment of VOCs..’

RACM2 and MCMv331 produce essentially the same P(O₃) for all but a few short time periods. This model difference is far from the focus of this paper. Therefore, we have dropped the discussion of these differences and their possible cause in order to keep the focus on the differences between the measured and modeled P(O₃) which is unaffected by these infrequent RACM2 – MCMv331 differences.

Pg 9, lines 6-16: The authors give some reasons as to why they have confidence in the MOPS measurements during the morning hours when the model and measurements do not agree. I am not convinced, however, that the MOPS measurements are not positively biased at this time: By removing the negative P(O₃) values which most frequently occurred during the morning hours, I would expect this to positively bias the measurements at this time even if a median rather than the mean value is used. Furthermore, I would expect heterogeneous HONO production to be greatest when NO₂ concentrations are high, and, this would also artificially positively bias the measurements during the morning most.

Please see comments for Reviewer 1 describing new correction techniques and providing evidence for the MOPS measurements being real in the mid-morning. Our additional analyses show that the MOPS diurnal pattern is rather robust for whichever correction to the raw P(O₃) data that we apply.

Please also see our comments above as to why we believe that HONO production (whether gas-phase or heterogeneous) is not a major issue in the MOPS chambers causing the measured P(O₃) to deviate from modeled P(O₃) in the morning. Deviations of P(O₃) from the average zero correction are seen in the MOPS raw data as stated in lines 15-17 on Pg. 6. These deviations from the MOPS raw data are greater than +3 ppbv/h: our calculated HONO bias from model simulations. If we account for the amount of HONO that could possibly be photolyzed during

the chamber residence time, this bias drops to less than 0.5 ppbv/h as mentioned above.

Pg 10, lines 1-5: The measurement bias reported due to photolytic HONO production is of the same magnitude as the discrepancy between model and measured P(O₃) observed during the morning (Fig 2). Although the authors argue that individual modelled and measured P(O₃) deviations are often larger than the bias caused by photolytic HONO production, there seems to be, from studying figure 1, a similar number of positive and negative deviations of the MOPS P(O₃) from the modelled P(O₃) suggesting that many of these deviations are caused by noise rather than missing or uncertain model chemistry.

Please see our comments for Reviewer 1 regarding the noise level on the MOPS data. By limiting the MOPS measurement time periods to those with ambient relative humidity below 70%, a majority of the observed P(O₃) noise is reduced. In addition, we average the MOPS data in Figure 1 in the main text to one hour. With this averaging, noisy data is also reduced and deviations from the hourly MOPS P(O₃) still exhibit differences relative to modeled P(O₃) that are larger than the HONO biases we estimate.

Section 3.3.4: A rate of $9-15 \times 10^{-11} \text{ cm}^3 \text{ molecule}^{-1} \text{ s}^{-1}$ for the postulated reaction 'OH+NO (+O₂) > HO₂ + NO₂' cannot be justified given that the known reaction rate for OH reacting with NO is two to three times slower. The impact of this highly speculative reaction is presented as positively influencing the modelled P(O₃) in line with the MOPS observations - this is misleading, however: Figure S2 highlights that although inclusion of this reaction, proceeding at a rate of $9-15 \times 10^{-11} \text{ cm}^3 \text{ molecule}^{-1} \text{ s}^{-1}$, improves the modelled and measured agreement in the morning, it actually worsens the agreement between the modelled and measured P(O₃) during the afternoon; there is no comment about this in the text, however. How does this reaction influence other modelled species, e.g. OH?

The reviewer is correct that the formation rate of the OH+NO adduct is known, but it has not been measured in atmospheric pressure air. It is possible that O₂ could act in some way to speed up this reaction. However, preliminary laboratory studies by us and another group and theoretical work have indicated that this reaction is unlikely to be fast enough even in the presence of oxygen. We have omitted this discussion as a possible explanation for the model-data mismatch discussed in this manuscript.

Section 3.3.6: Some discussion of the modelled HONO sources is needed here. If only gas-phase sources, i.e. OH+NO are considered, the model likely under-estimates the actual HONO that was present.

It is possible for the model to underestimate HONO. However, studies that have used measured HONO to constrain the models HONO still cannot resolve the HO₂ discrepancy at high NO_x, providing some evidence that a further HO₂ source at high NO_x may still be needed to resolve this issue. HONO levels needed to match the MOPS P(O₃) are a factor of two too high as

discussed in comments to Reviewer 1.

We have significantly modified section 3.3.4 on Pgs. 14-15 to discuss model HONO studies and sources of HONO present in the models used here.

Reference Tan et al., Atmos. Chem. Phys., 17, 663-690, 2017

This reference has been added to Pg. 4 in the Introduction.

Higher measured than modeled ozone production at increased NO_x levels in the Colorado Front Range

Bianca Baier^{1,a,*}, William Brune¹, David Miller¹, Donald Blake², Russell Long³, Armin Wisthaler^{4,5}, Christopher Cantrell⁶, Alan Fried⁷, Brian Heikes⁸, Steven Brown^{9,10}, Erin McDuffie^{9,10,11}, Frank Flocke¹², Eric Apel¹², Lisa Kaser¹², and Andrew Weinheimer¹²

¹Department of Meteorology and Atmospheric Science, The Pennsylvania State University, University Park, PA, USA

²School of Physical Sciences, University of California, Irvine, CA, USA

³US EPA National Exposure Research Lab, Research Triangle Park, NC, USA

⁴Institute of Ion Physics and Applied Physics, University of Innsbruck, Austria

⁵Department of Chemistry, University of Oslo, Norway

⁶Department of Atmospheric and Oceanic Sciences, University of Colorado Boulder, Boulder, CO, USA

⁷INSTAAR, University of Colorado Boulder, Boulder, CO, USA

⁸Graduate School of Oceanography, The University of Rhode Island, Kingston, RI, USA

⁹Chemical Sciences Division, NOAA Earth System Research Laboratory, Boulder, CO, USA

¹⁰Department of Chemistry and Biochemistry, University of Colorado Boulder, Boulder, CO, USA

¹¹Cooperative Institute for Research in the Environmental Sciences, University of Colorado Boulder, Boulder, CO, USA

¹²Atmospheric Chemistry Observations and Modeling Laboratory, National Center for Atmospheric Research, Boulder, CO, USA

^anow at: Cooperative Institute for Research in the Environmental Sciences, University of Colorado Boulder, Boulder, CO, USA and Global Monitoring Division, NOAA Earth System Research Laboratory, Boulder, CO, USA

Correspondence to: Bianca Baier (bianca.baier@noaa.gov)

Abstract. Chemical models must ~~accurately~~correctly calculate the ozone formation rate, $P(\text{O}_3)$, to accurately predict ozone levels and to test mitigation strategies. However, ~~model-chemical-mechanisms-can-contain-air-quality-models-can-have~~ large uncertainties in $P(\text{O}_3)$ calculations ~~;~~ which can create uncertainties in ozone forecasts; especially during the summertime when $P(\text{O}_3)$ ~~can-be-is~~ high. One way to test mechanisms is to ~~evaluate-model-compare-modeled~~ $P(\text{O}_3)$ ~~using-to~~ direct measurements.

5 During summer 2014, the Measurement of Ozone Production Sensor (MOPS) directly measured net $P(\text{O}_3)$ in Golden, CO, approximately 25 km west of Denver along the Colorado Front Range. Net $P(\text{O}_3)$ was compared to rates calculated by a photochemical box model ~~using-a-lumped-that-was-constrained-by-measurements-of-other-chemical-species-and-that-used-a-lumped-chemical-mechanism~~ and a more explicit ~~chemical-mechanism-Observed-one~~. Median observed $P(\text{O}_3)$ was up to a factor of two higher than that modeled during early morning hours when nitric oxide (NO) levels were high ~~;~~ ~~contrary-to-traditional-ozone-chemistry-theory~~. This disagreement may be due to model underestimation of hydroperoxyl ~~(and-was-similar-to-modeled-for-the-rest-of-the-day~~. While all possible interferences and offsets in this new method are not fully understood, ~~simulations-of-these-possible-uncertainties-cannot-explain-the-observed- $P(\text{O}_3)$ -behavior~~. Furthermore, atmospheric peroxy (HO_2) ~~radicals-relative-to-observations-at-high-NO-levels~~. These additional peroxy radicals could come from the MOPS chamber chemistry or from missing ~~and RO_2 radicals from unknown~~ volatile organic compounds co-emitted with nitrogen oxides

15 (NO_x ; ~~additional-cycling-of-OH-into- HO_2 -through-reactions-involving-nitric-oxide-provides-an-alternate-explanation-for-higher~~

~~measured than modeled~~) cannot fully explain the measured $P(O_3)$. ~~Although the MOPS measurements are new, comparisons of observed~~ This discrepancy observed between measured and modeled $P(O_3)$ ~~in NO space show a similar behavior to other comparisons between~~ is similar to those between measured and modeled peroxy radicals presented in this study and prior ones. If the MOPS accurately portrays atmospheric $P(O_3)$ ~~derived from measurements and modeled~~, then these results would imply that $P(O_3)$ ~~These comparisons can have implications for the sensitivity of in Golden, CO would be NO_x-sensitive for more of the day than what is calculated by models, extending the NO_x-sensitive $P(O_3)$ to nitrogen oxides and volatile organic compounds during morning hours, and can possibly regime from the afternoon further into the morning. These results could affect ozone reduction strategies for the region surrounding Golden, CO in addition to other urban and suburban and possibly other areas that are in non-attainment with national ozone regulations. Thus, it is important to continue the development of this direct ozone measurement technique to understand $P(O_3)$, especially under high NO_x regimes.~~

1 Introduction

Ground-level ozone (O_3) is a hazardous air pollutant abundant in cities and their surrounding areas. Awareness of its detrimental health effects on both humans and plants has led to the Clean Air Act of 1970 and the development of National Ambient Air Quality Standards (NAAQS) (Krupa and Manning, 1988; Bell et al., 2004; US EPA, 2013, 2016b). ~~These~~ Air pollution regulatory policies based on these standards have been successful in reducing O_3 by approximately 32% in the United States since 1980. However, current O_3 levels are stabilizing and even increasing again in the western United States (US EPA, 2016a). Understanding why these trends are occurring in areas despite more stringent emissions controls is crucial for further reduction of O_3 levels within the United States.

Boundary layer O_3 levels are dependent upon both chemical and meteorological processes described in the following equation:

$$\frac{\partial[O_3]}{\partial t} = P(O_3) + \frac{w_e \Delta O_3 - u_d [O_3]}{H} - \nabla \cdot (\mathbf{v}[O_3]), \quad (1)$$

where $\partial[O_3]/\partial t$ is the local O_3 time rate of change, $P(O_3)$ is the instantaneous net photochemical O_3 production rate, $(w_e \Delta O_3 - u_d [O_3])/H$ is the combined entrainment and deposition rate of O_3 in or out of the mixing layer of height H , and $\nabla \cdot (\mathbf{v}[O_3])$ is the O_3 advection rate. All of the physics, chemistry, and meteorology needed to solve this equation are included in chemical transport models (CTMs), which are used to design and test reduction strategies. For areas where local production is the dominant source of O_3 , the term in Eq. (1) that will reduce O_3 through local emissions control strategies is $P(O_3)$. Thus, understanding and accurately calculating O_3 formation is crucial for its mitigation.

Ozone formation chemistry has been well-documented for decades (Haagen-Smit et al., 1953; Finlayson-Pitts and Pitts, 1977; Seinfeld and Pandis, 2012; Calvert et al., 2015). The oxidation of volatile organic compounds (VOCs) by the hydroxyl radical (OH) produces hydroperoxyl-hydroperoxy (HO_2) and organic peroxyl-peroxy (RO_2) radicals. These peroxyl-peroxy

radicals react with nitrogen oxide (NO) to form nitrogen dioxide (NO₂), which is photolyzed to form new O₃ outside of the NO_x photostationary state (PSS): a steady-state reaction sequence involving NO_x (NO₂ + NO) and O₃. Thus, chemical O₃ production occurs through reactions with NO and ~~peroxy~~peroxy radicals described in Eq. (2), where k denotes a bimolecular reaction rate coefficient. Equation (3) describes the chemical O₃ (or NO₂) destruction rate or rate of removal to reservoir species as the fraction of O(¹D) molecules resulting from O₃ photolysis that react with H₂O to form OH; reactions of O₃ with HO_x (HO₂ + OH); the ~~production of organic nitrates P(RONO₂), including the~~ net production of peroxyacyl nitrates (PANs); the reaction of OH and NO₂ to form nitric acid (HNO₃); and O₃ loss through reactions with alkenes and halogens. The net instantaneous O₃ production rate, P(O₃), is then defined as the difference between O₃ chemical production and loss rates in Eq. (4) (~~Baier et al., 2015~~):

$$10 \quad P_{chem} = k_{NO+HO_2}[NO][HO_2] + \sum_{i=1}^N k_{NO+RO_{2i}}[NO][RO_2]_i \quad (2)$$

$$L_{chem} = J_{O_3} f_{H_2O}[O_3] + k_{OH+O_3}[OH][O_3] + k_{HO_2+O_3}[HO_2][O_3] + P(\del{RONO_2} \u{PANs}) + k_{OH+NO_2}[OH][NO_2] + L(O_3)_{alkenes} + L(O_3)_{halogens} \quad (3)$$

$$P(O_3) = P_{chem} - L_{chem}. \quad (4)$$

Equations (2) and (3) illustrate the non-linear dependence of P(O₃) on both NO_x and the production of HO_x from VOC oxidation. That is, these chemical species are involved in both the production and destruction of O₃ molecules. ~~Increases~~ According to the current understanding, increases in NO can cause P(O₃) to initially increase until NO_x levels are sufficiently high to react with OH, thereby removing HO_x and NO_x from the reaction system and decreasing P(O₃). Therefore, P(O₃) is largely dependent upon the cycling between HO_x and NO_x in the atmosphere; the exact NO_x level at which this crossover occurs is sensitive to the production rate of HO_x radicals (Jaegle et al., 1998; Trainer et al., 2000; Thornton et al., 2002; Ren et al., 2005). In a NO_x-sensitive regime, P(O₃) varies with the square root of P(HO_x) and decreases in NO_x are more effective in decreasing O₃ than decreases in VOCs. Conversely, in a VOC-sensitive regime, P(O₃) varies linearly with P(HO_x) and decreases in VOCs are more effective in decreasing O₃, while further NO_x decreases can act to increase O₃ (Kleinman et al., 1997; Seinfeld and Pandis, 2012). ~~If~~ Therefore, if the sensitivity of P(O₃) to NO_x and VOCs is known, efficient O₃ mitigation strategies can be devised that target precursor emissions and more effectively reduce O₃ in polluted regions.

The gas-phase chemical mechanisms used in CTMs rely on a number of model input parameters to calculate P(O₃) such as measurements of inorganic and organic chemical species; temperature- and pressure-dependent reaction rates; photolysis frequencies; and product yields of reactions. As the chemical processes contributing to O₃ formation are ~~both vast and complex~~,

vast, complex, and not fully quantified, it is difficult to portray atmospheric reactions in their entirety. Thus, mechanisms are simplified to describe the complex chemical state of the atmosphere. While inorganic chemistry is generally similar between reduced and more explicit mechanisms, differences in VOC aggregation schemes can create variance in modeled P(O₃), O₃,
5 or other important O₃ precursor predictions (Jeffries and Tonnesen, 1994; Olson et al., 1997; Kuhn et al., 1998; Luecken et al., 1999; Dodge, 2000; Tonnesen and Dennis, 2000; Jimenez et al., 2003; Luecken et al., 2008; Chen et al., 2010).

The ~~traditional view~~ current understanding of O₃ production chemistry is not consistent with all observations. ~~First, numerous~~
The production of O₃ is dictated by reactions between peroxy radicals (HO₂ and RO₂) and NO, but prior studies have
shown that measured and modeled peroxy radicals are not always in agreement. Stone et al. (2012) provide a synthesis of
10 model-measurement HO₂ comparisons, noting that model agreement with measurements is variable in low-NO_x environments,
but that models tend to underpredict HO₂ in urban, high-NO_x areas. Such studies in high-NO_x environments have shown that
both zero-dimensional and three-dimensional modeled HO₂ – or the HO₂ to OH ratio – ~~is underestimated~~ can be underestimated
by up to a factor of ten at values of NO greater than a few parts per billion by volume (ppbv) (Faloona et al., 2000; Martinez et al., 2003; Ren
~~although this underestimation was less severe and only evidenced above 20 ppbv in some studies due to significant VOC~~
15 ~~reactivity~~ (Shirley et al., 2006). ~~Nonetheless,~~ (Faloona et al., 2000; Martinez et al., 2003; Ren et al., 2003; Emmerson et al., 2005; Shirley
For some studies, the maximum NO values were approximately 6 ppbv (Tan et al., 2017), so that the amount of model
underestimation at high NO_x values was within measurement uncertainty. Other studies show good agreement between model
and measured HO₂ in the morning with average diel NO less than 2 ppbv (Hofzumahaus et al., 2009), or indicate good
20 average agreement between measured and modeled HO₂, but indicate morning model HO₂ underestimation on individual
days (Lu et al., 2013). In 2010, an interference involving partial conversion of RO₂ to HO₂ was found in HO₂ measurements
that use reagent NO to convert HO₂ to OH, so that measured HO₂ was overestimated (Fuchs et al., 2011). Since the publication
of that discovery, instruments are operated in a way that makes the interference negligible. However, even for measurements
prior to 2011, atmospheric HO₂/RO₂ ratios suggest that the magnitude of an HO₂ interference likely accounts for no more
25 than a factor of two in the difference between measured and modeled HO₂ (Cantrell et al., 2003). Removing this interference
therefore improves model-measurement HO₂ agreement, but cannot fully explain model HO₂ under-predictions at high NO_x
(Griffith et al., 2016; Brune et al., 2015; Tan et al., 2017).

Modeled organic peroxy radicals are also underestimated relative to measurements by up to a factor of ten (Hornbrook et al., 2011; Tan et
Tan et al. (2017) show that this underestimation can be most prominent at high NO_x and that further increasing a source
of morning RO₂ proportional to this discrepancy improves agreement between measured and modeled peroxy radicals, but
30 consequently overpredicts HO_x species or OH reactivity. Studies in which RO₂ (and/or HO₂) are underestimated via model
calculations at high NO_x have examined possible missing VOCs or additional mechanisms that could reconcile this effect, but
no such VOC or mechanism has been identified (Martinez et al., 2003; Kanaya et al., 2007; Dusanter et al., 2009; Hornbrook et al., 2011; L
To date, model under-prediction of peroxy radicals (either HO₂ or RO₂, and sometimes both species) at high NO_x levels
remains unresolved.

35 Due to the aforementioned discrepancies between measured and modeled radicals, P(O₃) calculated from measured ~~HO₂~~
peroxy radicals can routinely be more than double the P(O₃) calculated from modeled HO₂ (Kanaya et al., 2008; Ren et al., 2013; Brune et

~~Second, Im et al. (2015) and or RO₂ at high NO_x, according to several field studies conducted during the past decade (Ren et al., 2003; Kan~~
~~The Measurement of Ozone Production Sensor (MOPS) directly measures P(O₃) and can help to evaluate O₃ formation~~
~~calculated from chemical mechanisms via Eqs. 2-4 (Cazorla and Brune, 2010; Baier et al., 2015). However, observed P(O₃)~~
5 ~~has also shown similar discrepancies to modeled P(O₃) at high NO or NO_x. For example, in 2010 the first version of the~~
~~MOPS (Cazorla et al., 2012; Ren et al., 2013) compared directly-measured O₃ production rates to both modeled P(O₃) and that~~
~~calculated from measured peroxy radicals. Observed P(O₃) and P(O₃) calculated from measured radicals were approximately~~
~~equal to that modeled for NO levels up to 1 ppbv, but were significantly larger for higher values of NO.~~

~~Inaccurate model P(O₃) estimation can directly affect O₃ forecasts.~~ Im et al. (2015) and Appel et al. (2007) found that CTMs
10 ~~typically can~~ underestimate O₃ levels above 60-80 ppbv and overestimate O₃ below 30 ppbv: errors that are typically ~~accredited~~
~~credited~~ to emissions and chemical mechanism choice. ~~Summertime~~ ~~In addition, summertime~~ O₃ predictions were most sensi-
tive to regional production due to increased photochemical activity rather than transport (Im et al., 2015). ~~Finally, studies~~ ~~It has~~
~~also been found~~ in the northeastern United States ~~have shown that CTMs underestimate~~, that CTMs underestimated the effects
of NO_x emissions reductions on O₃ (Gilliland et al., 2008). Thus, ~~chemical mechanism uncertainties~~ ~~details of the chosen~~
15 ~~chemical mechanism~~ can greatly affect O₃ predictions and even reverse the order of O₃ production sensitivity to its precursors,
decreasing confidence in models used for developing emissions reduction strategies.

~~The Measurement of Ozone Production Sensor (MOPS) directly measures P(O₃) and can help to evaluate O₃ formation~~
~~calculated from chemical mechanisms (Cazorla and Brune, 2010; Baier et al., 2015). compared direct O₃ production rates to~~
~~both modeled P(O₃) and that calculated from measured peroxy radicals. Afternoon production rates were statistically similar~~
20 ~~between observed, calculated, and modeled P(O₃). In the early morning, MOPS P(O₃) magnitudes were similar to those~~
~~calculated from measured radical species, but were almost twice as large as modeled rates. Similarly, observed P(O₃) and that~~
~~calculated from HO₂ observations were approximately equal to that modeled for NO levels up to 1 ppbv, but were significantly~~
~~larger for higher values of NO (Ren et al., 2003; Spencer et al., 2009; Ren et al., 2013; Cazorla et al., 2012; Brune et al., 2015).~~

25 ~~P(O₃)~~ was measured in Golden, CO in ~~Summer~~ ~~summer~~ 2014 during ~~a field study consisting of~~ the Deriving Information
on Surface conditions from Column and VERTically-resolved observations Relevant to Air Quality (DISCOVER-AQ) field
campaign and the Front Range Air Pollution and Photochemistry Experiment (FRAPPÈ). This ~~paper work~~ describes compar-
isons between P(O₃) measured ~~in situ~~ ~~in situ~~ by a second-generation MOPS and ~~modeled~~ P(O₃) ~~modeled~~ using both lumped
and near-explicit chemical mechanisms. ~~Finally, we examine and we investigate the~~ possible causes for differences observed
30 between measured and modeled P(O₃).

2 Methods

2.1 MOPS measurements

A second-generation MOPS directly measures the instantaneous O₃ production rate, P(O₃), with an improved chamber and
airflow design. The method is briefly described here; a more ~~thorough~~ technical description of the MOPS and its modifications

is detailed in Baier et al. (2015). The second-generation design aims to decrease artificial chemistry induced by air-surface interactions within the chambers. The difference in O_x (defined here as $O_3 + NO_2$) is continuously sampled by two 26.9-L trapezoidal environmental chambers with airflow somewhat like a sheath flow to isolate sampled air from chamber surfaces. ~~A~~The sample chamber is transparent and undergoes the same O_3 photochemistry as the atmosphere, while ~~a~~the reference chamber is covered with a film that blocks all ultraviolet (UV) radiation of wavelengths below 400 nm, suppressing the radical chemistry essential for new O_3 production. Positioned after the chambers, a highly-efficient UV light-emitting diode photolyzes NO_2 into O_3 in air coming through separate tubing from both the sample and reference chambers. This converter cancels any differences in the NO_x PSS caused by the reference chamber film. The difference in O_x , divided by the exposure time of air in the MOPS chambers, yields the net O_3 production rate as $P(O_x)$.

The residence time is determined by adding a pulse of O_3 to the chambers and then measuring the O_3 as a function of time (Baier et al., 2015). The resulting pulse has a mean residence time of 130 ± 5 s and the time at which the signal recedes into the background is 345 s. Thus, the exposure time of molecules in the chambers is taken to be 130 s.

The MOPS absolute uncertainty (1σ) is ± 11 ppbv h^{-1} for 10-min measurements (Baier et al., 2015). ~~At times, but when averaged to one hour, this uncertainty decreases to approximately 5 ppbv h^{-1} . As previously mentioned in Baier et al. (2015), the MOPS measures artificial positive and technique can produce artificial negative O_3 production rates. Like previous discussion that are roughly correlated with temperature, relative humidity, or actinic flux. As discussed in Cazorla et al. (2012), negative $P(O_3)$ rates are unrealistic during the day when OH production is large enough to sustain new NO_2 and subsequent O_3 formation from VOC oxidation. Anomalous positive $P(O_3)$ is sometimes measured before sunrise or in the early morning, also indicating possible artifacts in the MOPS measurements.~~

MOPS chamber loss tests and flow visualizations have indicated been conducted to address these artifacts. Laboratory testing indicates that wall loss of O_x is negligible (Cazorla and Brune, 2010; Baier et al., 2015). Although the MOPS and radical species is minimal (Cazorla and Brune, 2010; Baier et al., 2015). On the other hand, previous studies have found that commercial O_3 analyzers can exhibit both positive and negative responses to changes in relative humidity due to increases or decreases in water vapor (US EPA, 1999; Wilson and Birks, 2006). Additional laboratory testing has been conducted to investigate the sensitivity of the MOPS Thermo Scientific O_3 analyzer used in this study. Although differences in temperature between sample and reference chamber did not play a large role in initiating baseline drifting, the MOPS O_3 analyzer exhibits a large baseline shift greater than approximately 2 ppbv when the ambient relative humidity is greater than 70%.

The MOPS precision is typically 5 ppbv h^{-1} (1σ), for one-hour averages, but O_3 analyzer drifting can degrade this precision. Random, non-linear analyzer drifting occurs during the day and, like previous studies, is hypothesized to stem from humidity differences between the UV absorption cells in the MOPS Thermo Scientific. We quantify the MOPS diurnal O_3 analyzer drift and provide a correction to the raw $P(O_3)$ analyzer (US EPA, 1999; Wilson and Birks, 2006; Baier et al., 2015). Drifting is partially corrected through zeroing) data through zeroing of the MOPS chambers, either by removing the reference chamber film for an entire day, or by measuring $P(O_3)$ on cooler, cloudy days when O_3 formation is likely near zero (Baier et al., 2015). low (Baier et al., 2015). On these occasions, the negative O_3 differential due to high relative humidity is apparent. Since the same O_3 formation will occur in both chambers on these occasions zero days, this method should retrieve a "zero" retrieves

5 a baseline $P(O_3)$ time series that can be subtracted off of the MOPS raw data. ~~However, this zero only partially corrects for this drifting due to varying humidity from day to day. Consequently, the corrected MOPS baseline routinely drifts between -5 and 5 ppbv hr^{-1} most mornings and late afternoons when~~ Four zeros were applied to the raw $P(O_3)$ data during this study for an entire 24-hour period, with two using low O_3 production days as zeros. Positive deviations in the MOPS raw $P(O_3)$ from this negative baseline are evident during the morning hours, therefore this method extracts the positive $P(O_3)$ deviations from background O_3 analyzer drift during O_3 production hours of the day. Zeros that were taken only on days with diurnal patterns and absolute values of relative humidity that are similar to most MOPS measurements days were used in this analysis. The average zero correction that is subtracted from the raw $P(O_3)$ measurements to derive a corrected MOPS $P(O_3)$ is typically low, shown in Fig. S1. In addition, we have restricted our analysis to days when the ambient relative humidity was below 70% and have tested the robustness of this threshold using a wide range of relative humidities from 70%-90% to ensure that our corrected $P(O_3)$ values were not sensitive to this threshold choice (Fig. S2).

15 The MOPS chamber "sheath" airflow ~~deters species adsorption (desorption) to (from) surfaces with high flow rates of approximately 20 LPM along the walls of the chambers~~ inhibits air that has contacted the walls from being sampled in the center of the chamber exit (Baier et al., 2015). Air is then sampled from a slower, center flow that is isolated from the chamber walls. Smoke visualizations of the chamber flow, along with laboratory and atmospheric observations of chamber O_x losses less than or equal to 5%, suggest that off-gassing of O_x or other species from the MOPS chamber walls is inhibited and thus likely plays a negligible role in larger measured-than-modeled $P(O_3)$. From the laboratory and chamber testing to date, insignificant amounts of NO are lost in the MOPS chambers (Cazorla and Brune, 2010; Baier et al., 2015).

20 It is known that NO_2 adsorption onto the chamber walls can result in the heterogeneous formation of nitrous acid (HONO) through the reaction of NO_2 with water vapor adsorbed onto surfaces (Finlayson-Pitts et al., 2003). ~~A~~; a photolytic HONO source has also been previously reported (Rohrer et al., 2005; George et al., 2005; Stemmler et al., 2006; Langridge et al., 2009; Lee et al., 2016; Crilley et al., 2016). During the 2013 DISCOVER-AQ study in Houston, TX, ~~some excess HONO~~ excess HONO of up to five times ambient values was measured in the MOPS chambers, which can thus create excess OH and positively bias the MOPS $P(O_3)$ ~~production. This HONO source has been~~. Although a production mechanism has not been identified, this bias was found to be a) largest between 1000-1400 LT when NO_x values are high, and b) correlated with relative humidity, temperature, and J_{NO_2} ~~and actions were taken prior to DISCOVER-AQ 2014 to reduce this measurement~~ (Baier et al., 2015). The MOPS inlet is one area that is suspected to facilitate HONO production due to inevitable surface interactions with sample air entering the chambers, and we have since decreased this bias by approximately 30%. ~~We calculate that this artifact reflects a maximum 3.5-7 ppbv h^{-1} positive bias in observed~~ through shielding the MOPS inlet face and suppressing additional HONO production. Chamber HONO values measured in Houston, TX were applied to this Golden, CO study by scaling the observed chamber HONO by the ambient NO_x ; then the possible $P(O_3)$ for this study. The bias and random errors are incorporated into a propagation of uncertainty analysis in order to calculate the MOPS absolute uncertainty (Baier et al., 2015) ~~interference due to chamber HONO was determined.~~

2.2 Site description and ancillary measurements

Second-generation MOPS measurements were recorded for 19 days in Golden, CO (39°44.623'N, 105°10.679'W), which is located approximately 25 km west of the Denver metropolitan area. Commerce City, which houses several oil refineries, is located 30 km to the northeast. The Golden measurement site lies east of the Front Range, atop the South Table Mountain mesa (1833 m asl) and amidst grass-covered terrain. The Colorado summertime climate is hot and arid with intense solar radiation. These meteorological conditions can be conducive for high O₃ formation from both local and advected precursor emissions. Ozone production can also be affected by diurnally varying, thermally driven winds; morning heating of mountains invokes easterly upslope flow, transporting precursors from Denver and the urban corridor of the Front Range westward, while downsloping afternoon westerlies can re-circulate these pollutants eastward to lower elevations (Banta, 1984).

Measurements used to constrain the models in this study were obtained on ground-based and aircraft platforms during DISCOVER-AQ and FRAPPÉ. Both studies were co-located in the Colorado Front Range between 17 July and 10 August 2014. Continuous, ground-based 1-min measurements of meteorological parameters and inorganic chemical species include temperature, pressure, and relative humidity, O₃, sulfur dioxide, and NO_x. In the absence of continuous ground-based VOC measurements, C₂-C₁₀ non-methane hydrocarbons (NMHC) and organic nitrates were measured from 72 total whole-air canister (WAC) samples that were collected in Golden and analyzed by gas chromatography (GC) and gas chromatography-mass spectrometry (GC-MS) in the laboratory. ~~A daily~~ An average of five samples were taken daily over 16 days, ~~with heavier sampling~~. Approximately 64% of whole air sampling occurred between 0700 and 1200 local time (LT) to capture VOC mixing ratios during morning O₃ production hours, ~~and with~~ sparser sampling in the afternoon between 1400 and 1800 LT to examine advection from areas-sources east of Golden, CO such as the Denver metropolitan ~~region and the Commerce City region~~ and Commerce City regions. Median diurnal values of VOCs were constructed from these point measurements to provide constraints for the model calculations. ~~In addition, we~~ We initialized backward Hybrid Single-Particle Lagrangian Integrated Trajectory (HYSPLIT) models at 300 and 500 m heights beginning at 1600 LT and run for 12 hours using North American Model (NAM) meteorological data to determine whether the airflow in Golden could have originated from these eastern regions (Stein et al., 2015; Rolph, 2016). In general, higher NO_x and anthropogenic VOC mixing ratios were measured when HYSPLIT indicated flow from these eastern pollution sources. ~~For~~ Thus, for days when measurements were made in these plumes, separate median diurnal VOC values were constructed to more accurately represent the VOC speciation observed in Golden.

Canister VOCs were supplemented by boundary layer inorganic and organic chemical species measurements obtained on the NASA P-3B and NSF/NCAR C-130 aircraft and constant, median values were calculated for ~~times when the~~ the limited times of the day when these aircraft were in the vicinity of Golden and used in the model (Table 1, Table S1). ~~Measurements aboard the Aircraft measurements for Golden were available after 0900 LT on P-3B were used when it was directly overhead of Golden, CO, overflights which occurred up to three times daily,~~ while C-130 measurements were ~~used~~ available after 1000 LT when this aircraft was within roughly 20 km of the measurement site. Airborne measurements of inorganic and organic species agree to within 30% on average. More information on the DISCOVER-AQ and FRAPPÉ campaigns, aircraft and ground-based

platforms, and measurement methods can be found at <http://www-air.larc.nasa.gov/missions/discover-aq/discover-aq.html> and <https://www2.acom.ucar.edu/frappe>.

2.3 Model description

5 Two types of chemical mechanisms were used in zero-dimensional photochemical box models to calculate $P(O_3)$ for the **entire** DISCOVER-AQ and FRAPPÉ campaign period. We used the lumped Regional Atmospheric Chemistry Mechanism version 2 (RACM2) (Stockwell et al., 1997; Goliff et al., 2013), and the near-explicit Master Chemical Mechanism version 3.3.1 (MCMv331) (Jenkin et al., 2003; Bloss et al., 2005; Jenkin et al., 2015). An exhaustive list of model constraints is displayed in Table 1. Cloud-free photolysis rates were calculated using the Tropospheric Ultraviolet (TUV) model (Madronich and Flocke, 10 1999) for Golden, CO. These photolysis rates were scaled to J_{NO_2} calculated from continuous pyranometer measurements (LI-COR, LI-200 series) using the relationship described in Trebs et al. (2009) and then were used to constrain the models. All model constraints were interpolated to a 10-minute time step and input into the model to calculate $P(O_3)$ for the campaign period. The system of differential equations generated from both chemical mechanisms was integrated for 24 hours to allow reactive intermediates to reach steady-state. In addition, ~~longer-lived inputs not constrained by a one-day integration time~~ 15 is calculated to be sufficient for radical concentrations and intermediate species to reach steady-state as a two-fold or even three-fold increase in this integration time period did not impact radical concentrations or the $P(O_3)$ results described below. Longer-lived constituents not constrained in the model were given a 24-hour lifetime to both prevent buildup of these chemical species and to roughly account for advection or dilution losses. Modeled $P(O_3)$ is largely insensitive to this loss rate. We note that ~~although transport and entrainment processes can also influence O_3 levels, zero-dimensional model runs described here~~ 20 ~~do not include these processes. Instead, we focus on net $P(O_3)$, ~~which is~~ calculated with Eqs. 2-4 using modeled output.~~

2.4 Model uncertainty assessment

In order to explain calculated $P(O_3)$ behavior relative to the MOPS during hours of the day when there is typically a shift from VOC- to NO_x -sensitive $P(O_3)$ regimes, we explore model sensitivity to various inorganic and organic chemical species, reaction rates, product yields, and other model parameters outlined in supplementary material. For cases in which modeled 25 O_3 sensitivity is near the transition between VOC-sensitive and NO_x -sensitive, model $P(O_3)$ uncertainty can mask the proper designation of O_3 NO_x -VOC sensitivity (Chen and Brune (2012) and references therein). Thus, understanding the uncertainty of modeled $P(O_3)$ to model inputs and parameters defines what can be said about modeled O_3 sensitivity to VOCs and NO_x .

2.4.1 RACM2

The RACM2 model includes 119 species and 363 reactions ~~and~~ and is run using the FACSIMILE solver (Stockwell et al., 1997; 30 Goliff et al., 2013). An explicit isoprene chemistry scheme has replaced the original RACM2 isoprene chemistry ~~and~~ and is highlighted in Paulot et al. (2009) and Mao et al. (2013). As this mechanism aggregates VOCs based on their functional

groups and OH reactivity, the RACM2 significantly reduces the number of model inputs and parameters over more explicit mechanisms that treat VOCs and their intermediate products separately.

Model uncertainty is traditionally evaluated through sensitivity analyses in order to identify inputs (observational data) and parameters (reaction rates and product yields) that create the most variance in a model output of interest. These inputs are hereby called “influential” inputs. The RACM2 model uncertainty is assessed through the use of a global sensitivity analysis for daylight hours between 0600 and 1800 LT.

A Random Sampling-High Dimensional Model Representation (RS-HDMR) analysis was performed, which varies hundreds of model constraints with relatively low computational expense (Rabitz and Alis, 1999; Li et al., 2006, 2010). The variance in modeled $P(O_3)$ due to changes in influential model constraints was calculated, with the $P(O_3)$ 1σ uncertainty derived as the total $P(O_3)$ standard deviation divided by its mean from time periods evaluated between 0600 and 1800 LT. The RS-HDMR technique used for the RACM2 model runs is detailed in Chen and Brune (2012) and Chen et al. (2012). An overview of model input uncertainties and a description of this global sensitivity analysis are presented in supplementary documentation.

2.4.2 MCMv331

The MCMv331 (Jenkin et al., 1997; Saunders et al., 2003; Bloss et al., 2005; Jenkin et al., 2015), is freely available at <http://mcm.leeds.ac.uk/MCM> and is run using a MATLAB framework described in ~~Wolfe et al. (2011)~~ [Wolfe et al. \(2016\)](#). This mechanism includes roughly 6,000 species and 17,000 reactions, treats VOCs and their intermediates separately, and uses explicit isoprene degradation chemistry described in Jenkin et al. (2015). Because of the large number of inputs in this near-explicit mechanism, the MCMv331 uncertainty was assessed through a local sensitivity approach. That is, inputs were set to their upper and lower uncertainty limits ([at a \$1\sigma\$ confidence level](#)) in a one-at-a-time fashion while all other constraints were held at their original values. Total MCMv331 uncertainty was calculated by adding in quadrature the upper and lower percent deviations in $P(O_3)$ due to perturbations in model constraints relative to the MCMv331 base case. Input and parameter groups that were varied to derive this uncertainty are described in supplemental documentation.

3 Results

3.1 Campaign observations and $P(O_3)$ time series

Observed and modeled $P(O_3)$ were compared ~~for 19 days~~ between 17 July and 10 August 2014 in Golden (Fig. 1). From 17-27 July, the campaign was characterized by a warmer, drier period followed by a relatively cooler, wetter period until the end of the study. Daily O_3 mixing ratios typically peaked between 1300-1800 LT with a median value of 59 ppbv. Higher O_3 levels exceeding 80 ppbv were observed on 22, 28, and 29 July as well as 3 August. The highest O_3 levels were observed on 22 July with a maximum mixing ratio of approximately 90 ppbv.

Due to the terrain of the Front Range, the average diel wind direction during the campaign period was westerly before 0900 LT, easterly to northeasterly from 0900 to 1400 LT, and then westerly again after 1400 LT, with ~~diel~~ [diel-averaged](#) speeds

ranging between 2-3.5 m s⁻¹. Thus, it is possible for P(O₃) in Golden can to be influenced by pollutants advected from nearby eastern source regions during the mid-morning to early afternoon.

The corrected MOPS P(O₃) maxima were routinely higher than 10 ppbv h⁻¹ on most measurement days, with diurnal peaks between 0900-1100 LT. Observed P(O₃) maxima on individual days range from 10 ppbv h⁻¹ to almost 40-30 ppbv h⁻¹ (Fig. 1). ~~Observed baseline P(O₃) values were typically between -5 and 5 ppbv h⁻¹. However, the MOPS measured As mentioned earlier, MOPS P(O₃) less than -10 ppbv h⁻¹ on some early mornings and late afternoons. These negative values are likely due to our inability to correct for measurements were restricted to days when the ambient relative humidity is less than 70% when we have confidence that the O₃ analyzer drifting, which is exaggerated by high humidity or drastic changes in humidity during the measurement period. To account for possible anomalous P(O₃) measurements due to humidity or its changes, MOPS data during these time periods have been removed from this analysis. Despite this artifact, MOPS variations were generally consistent with observed diurnal O₃ variations, with higher P(O₃) measured on days where O₃ mixing ratios were greater than 70 ppbv (Fig. 1). was not affected by significant baseline drifting. This data filtering reduced the MOPS baseline variations to between -5 and 5 ppbv h⁻¹ at a 1-hour time resolution.~~

3.2 Modeled P(O₃) time series and comparisons to measurements

Full-campaign modeled P(O₃) is also shown in Fig. 1 for both RACM2 and MCMv331. Modeled P(O₃) ~~maxima were exhibited for both mechanisms are a broad peak with maxima that occurred~~ between 0900-1200 LT with values generally 10 ppbv h⁻¹ or lower. The modeled P(O₃) ~~variations, however, were not always consistent with O₃ variations, with some of the highest P(O₃) calculated for rather low O₃ days (20-21 July and 25 July). The behavior is essentially identical on a day-to-day basis for both the RACM2 and MCMv331~~ P(O₃) behavior was similar throughout the campaign period although occasionally, the ~~MCMv331. On several individual days, the MOPS P(O₃) indicated spikes throughout the day where the RACM2 did not. This result is perhaps due to the more explicit treatment of VOCs and their intermediate products in the MCMv331 versus the RACM2. Nonetheless, the RACM2 generally produces measurements exhibited maxima that were a factor of two to three times higher than modeled P(O₃) patterns similar to that produced by the more explicit MCMv331 values during the morning between 0900-1100 LT.~~

~~In Fig. 2, median~~ Median diel variations of MOPS and modeled P(O₃) are shown for MOPS measurement days ~~Indicated by the 25th, median, and 75th percentiles, in Fig. 2. Median~~ observed P(O₃) began to increase around 0800 LT, ~~was highest from 0900-1100 LT and then decreased later in the day. Modeled 5 ppbv h⁻¹ before falling off to zero in the evening. Median modeled P(O₃) generally followed the same diurnal pattern and was in rough agreement with the MOPS in the afternoon. Measured also rose beginning at about 0800 LT but peaked at around 5 ppbv h⁻¹ between 1100 and 1200 LT, and was 3-4 ppbv h⁻¹ in the afternoon. Median observed and modeled P(O₃), however, were less similar during early morning peak~~ are in good agreement in the afternoon as shown by overlapping errorbars, but median diel MOPS P(O₃) hours is generally a factor of two higher than that modeled between 0900-1100 LT when NO_x and VOC levels were higher-high due to abundant local and-or advected rush hour traffic emissions. The majority of the MOPS shaded region in Fig. 2 is the range of possible measured P(O₃) values obtained using the range of maximum to minimum

35 measured zero offset values. This mid-morning difference between measured and modeled diel-averaged P(O₃) measurements exhibited maxima that are up to a factor of two higher than is apparent over this range of zero corrections.

Figure 5 indicates P(O₃) as a function of NO levels and time of day. Similar to Cazorla et al. (2012), both measured and modeled diel P(O₃) increased between 0600-0800 LT during morning rush hour, peaked before 1200 LT, and then decreased later in the day with decreasing NO and VOC radical abundances. Occasional secondary P(O₃) peaks were exhibited between 1400-1600 LT in both measured and modeled P(O₃), likely due to advection of O₃ precursors from the Denver region or increased local traffic emissions. The most striking difference is that the measured P(O₃) continues to rise as NO increases while the modeled P(O₃) decreases for NO more than 1 ppbv. The missing modeled P(O₃) values during this time period appears to increase monotonically with increasing NO for NO values greater than roughly 1 ppbv (Fig. 4). The difference between measured and modeled P(O₃) is near zero up to 1 ppbv NO and almost 15 ppbv h⁻¹ at 5 ppbv NO. This unexpected increase in P(O₃) with increasing NO provides a clue as to what might be causing the difference between measured and modeled P(O₃).

Several reasons provide confidence in these P(O₃) comparisons, which result in higher P(O₃) than that modeled during the morning hours despite the MOPS absolute uncertainty. First, median P(O₃) values were used instead of the mean to compare MOPS and modeled P(O₃) so as not to bias diurnal P(O₃) curves high or low in the event of P(O₃) anomalies. Next, the second, observed P(O₃) peak values were often much greater than the hourly MOPS 1σ uncertainty shown on individual days as seen in Fig. 2 was relatively independent of time of day. That is, this uncertainty acts as an offset, shifting the entire median diurnal curve, where differences between the MOPS and modeled P(O₃) were typically between 10-20 ppbv h⁻¹. Third, when different relative humidity thresholds are used to correct the raw P(O₃) curve either up or down, but data, measured P(O₃) consistently exhibits the same diurnal behavior relative to the models. This result was observed for a range of atmospheric conditions: for both hot, dry and cool, high humidity days as well as for higher and lower NO days. For low NO days (NO ≤ 1 ppbv), median with a positive deviation from modeled P(O₃) between the MOPS and models were in closer agreement, but MOPS P(O₃) around 1000 LT. Fourth, deviations from the modeled P(O₃) still exhibited maxima before that modeled in the early morning. Finally, the observed differential baseline derived from zeroing methods are observed between 0900-1100 LT even before correcting the MOPS measurements. Thus, we have confidence in the positive MOPS P(O₃) peak values were often much greater than the MOPS 1σ absolute uncertainty on individual days as seen in Fig. 1, where differences between the MOPS and modeled P(O₃) were typically between 10-20 ppbv h⁻¹. Thus, all during the morning hours. All of these results provide confidence in the robustness of the MOPS behavior relative to the models in Figs. 1 and 2 and in the subsequent analyses.

3.3 **Model-measurement Possible causes of the model-measurement P(O₃) discrepancies**

3.3.1 **MOPS chamber artifacts**

30 Higher morning P(O₃) calculated from measured peroxy radicals has been observed at high NO with a variety of measurement methods. The MOPS observations, independent of these studies, yield similar results for the dependence of P(O₃) on NO indicating that either all of these measurement methods contain similar artifacts, or that model-measurement disagreement

occurs due to differences in the chemistry between observational and computational methods used to determine O₃ production rates.

We explore several ~~reasons~~ hypotheses for model-measurement disagreement during the morning hours ~~in the following sections.~~ Possible explanations include MOPS chamber artifacts, model input and parameter uncertainties, model peroxy radical chemistry, modeled ambient HONO sources, and reactive chlorine chemistry.

3.3.1 MOPS chamber artifacts

One hypothesis is that the MOPS P(O₃) is positively biased due to environmental chamber chemistry artifacts: that is, ~~offgassing~~ off-gassing of NO₂, HONO, or other chemical species from the chamber walls. At higher relative humidity, chemical species adsorption onto these environmental chamber walls can be higher (Wainman et al., 2001) ~~and it.~~ It is possible that subsequent desorption of NO₂ or chemical species from the walls can induce artificial chemistry in the MOPS chambers.

~~Wall effects in the MOPS chambers can create both positive and negative fluctuations in observed P(O₃).~~ However, as described earlier, the MOPS chamber airflow ~~is significantly higher along isolates sampled air from~~ the walls of the MOPS chambers where surface reactions are most likely to occur. ~~All-chamber~~ Chamber air closest to the walls is exhausted, leaving mostly center flow to be sampled by the MOPS O₃ analyzer. ~~This airflow design, along with laboratory and atmospheric observations of chamber O_x losses less than or equal to 5%, suggests that off-gassing of O_x or other species from the MOPS chamber walls likely plays a negligible role in larger measured than modeled P(O₃) (Cazorla and Brune, 2010; Baier et al., 2015). From the laboratory and chamber testing to date, a significant loss of NO in the MOPS chambers has not been identified. Additionally, while~~

Additionally, adsorbed NO₂ can result in heterogeneous formation of nitrous acid (HONO), and a ~~photolytic~~ HONO source within the chambers ~~can also may~~ result in excess P(O₃) from artificial OH production (Baier et al., 2015), ~~we calculate that this artifact during the 2014 DISCOVER-AQ campaign yields a maximum bias (3.5-7.~~ For the Golden, CO study, NO_x levels were a factor of three lower on average than in Houston, TX, the relative humidity was 35% lower on average, and the actinic flux was similar. Therefore, we have applied the observed chamber HONO:NO_x ratio in Houston, TX to the Golden, CO study because the HONO production should depend linearly on NO_x adhering to the walls. We have calculated a maximum diurnal bias of +3 ppbv h⁻¹) that is substantially lower than most daily MOPS P(at 1000 LT (2σ) that decreases later in the day to less than 1 ppbv h⁻¹ as NO_x decreases. However, this calculated bias is rather conservative; the chamber residence time of 130 s and the HONO photolysis frequency for Golden, CO can be used to determine the percentage of chamber HONO that would be converted into O₃) deviations from modeled-producing radicals. In doing so, less than 15% of chamber HONO is photolyzed. Thus, the bias for Golden, CO would be less than 0.5 ppbv h⁻¹ and would contribute insignificantly to the observed P(O₃) observed in Fig. 1. Therefore, in signal. In order to explain observed and modeled P(O₃) differences, ~~excess P(O₃) from HONO production at Golden by chamber-produced HONO, levels would need to be approximately three to five times larger than has been observed within the MOPS chambers. As mentioned earlier, higher morning more than an order of magnitude larger. Therefore, the likelihood of chamber-induced P(O₃) calculated from measured HO₂ has been observed at high NO with a variety of measurement methods. The MOPS observations are independent of these previous studies, but yield~~

~~similar results for the dependence of from excess HONO production causing differences between observed and modeled P(O₃) on NO, providing confidence that higher observed is small.~~

3.3.2 Model input and parameter uncertainty

5 ~~A second hypothesis is that the uncertainties in the model P(O₃) is not due to significant chamber artifacts, but instead to possible are large enough that the differences in the chemistry between models and the MOPS measurements.~~

3.3.3 **Influential model parameters**

~~measured and modeled P(O₃) are not statistically different. Model P(O₃) uncertainty has been found to be slightly 2-5% larger during the morning hours when differences between measured and modeled P(O₃) were observed. Furthermore, model P(O₃) uncertainty can possibly shift the designation of O₃-NO_x-VOC sensitivity (Chen and Brune (2012) and references therein). In order to explain calculated P(O₃) behavior relative to the MOPS during hours of the day when there is typically a shift from VOC to NO_x-sensitive P(O₃) regimes, we explore model sensitivity to various inorganic and organic chemical species, reaction rates, product yields, and other model parameters outlined in supplementary material.~~

As described earlier, the RACM2 inputs and parameters affecting model P(O₃) uncertainty are determined based on a RS-
15 HDMR sensitivity analysis. Model uncertainty between 0600 and 1800 LT is similar between both chemical mechanisms (Table S4); the average modeled P(O₃) uncertainty (1σ) from RACM2 and MCMv331 ~~is highest between 0600-1200 LT with a 1σ value of 31%, and decreases slightly to 29% between 1200 and 1800 LT. Thus, due about 30% all day. Due~~ to similar model behavior and diurnal uncertainty estimates between the RACM2 and the MCMv331, we expect that the influential inputs between the two mechanisms – model constraints and parameters contributing largely to calculated P(O₃) uncertainty – will
20 also be similar.

Model influential inputs are specific to both location and available measurements. However, many constraints that contributed to P(O₃) uncertainty in Golden, CO were found to be similar to prior sensitivity analyses of chemical mechanisms conducted in much different environments (Chen and Brune (2012) and references therein). For example, two parameters consistently identified as having high importance for daytime P(O₃) uncertainty involve the reaction rates, k_{OH+NO_2} and
25 k_{HO_2+NO} , which dictate HO_x-NO_x cycling and the production and loss of HO_x. ~~Thus, even though the uncertainty factors for these parameters are relatively low at~~ These reaction rate coefficients have large contributions to the overall model uncertainty despite their relatively low uncertainty factors of 1.3 and 1.15 respectively (Sander et al., 2011), this important result suggests that greater emphasis should be placed on quantifying the uncertainty in HO_x-NO_x cycling reaction rates to reduce model P(O₃) uncertainty.

30 Other model constraints influential in dictating model P(O₃) uncertainty such as reaction rates, product yields and mixing ratios of species were more specific to time of day. Similar to overall results in Chen and Brune (2012), and in addition to HO_x-NO_x reaction rates, early morning P(O₃) uncertainty was attributed to reaction rates involving the oxidation of reactive VOCs such as aldehydes and xylenes that initiate O₃ formation propagation and produce HO_x. Additional Golden influential reaction rates involved the decomposition and formation rates of peroxyacyl nitrates (PAN), a NO_x reservoir. As O₃ increases

in the afternoon, additional rates and product yields of reactions involving O_3 loss also become important, along with those between NO and other organic ~~peroxy+peroxy~~ species (RO_2) that continue O_3 formation.

As expected, model inputs and parameters involving the formation of RO_2 or new NO_2 outside of the NO_x PSS that further propagate the O_3 formation cycle, along with inputs and parameters involving production of HO_x species, are all factors influencing model $P(O_3)$ uncertainty. ~~Therefore, although~~ Although model uncertainty is not large enough to explain model $P(O_3)$ behavior relative to the MOPS, ~~decreasing uncertainty in model inputs, especially~~ greater emphasis should be placed on quantifying the uncertainty in HO_x - NO_x reaction rates, ~~may help to decrease total cycling reaction rates to reduce~~ model $P(O_3)$ uncertainty and improve morning agreement between observed and modeled $P(O_3)$ in Figs. 1 and 2.

3.3.3 ~~HO₂ versus NO~~ Model peroxy radical chemistry

~~Model chemistry plays a large role in calculated~~ One hypothesis for lower modeled $P(O_3)$ ~~uncertainty. Therefore, we examine the chemical features driving early morning modeled-to-measured $P(O_3)$ discrepancies in the early morning is that modeled HO_2 is underestimated at high NO. Indeed, in previous studies, measured HO_2 often exceeds modeled HO_2 for NO greater than about 1 ppbv (Faloona et al., 2000; Martinez et al., 2003; Ren et al., 2003; Shirley et al., 2006; Emmerson et al., 2007; Kanaya et al., 2007) Campaign median NO mixing ratios typically peaked between 0900-1100 LT at about 2 ppbv with maxima as high as 7 ppbv.~~ As the The largest differences in measured and modeled $P(O_3)$ occur during this time period when NO is greater than 1 ppbv; ~~and HO_x - NO_x cycling reactions are significant in dictating model.~~ Thus, it is possible that the difference between measured and modeled HO_2 is related to the difference between measured and modeled $P(O_3)$ uncertainty, we first examine cycling of HO_x as a function of NO.

Measurements of HO_2 and ~~OH~~ HO_2 (35% accuracy, 2σ) and OH (45% accuracy, 2σ) were made on board the NSF/NCAR C-130 using chemical ionization mass spectrometry (CIMS) ~~with 35% and 45% accuracy (2σ), respectively (Mauldin et al., 2003; Hornbrook et al., 2003).~~ One hypothesis for lower modeled $P(O_3)$ in the early morning is that modeled HO_2 is underestimated at high NO. Similar to prior studies (Faloona et al., 2000; Martinez et al., 2003; Ren et al., 2003; Shirley et al., 2006; Emmerson et al., 2007; Kanaya et al., 2007; Fig. (Mauldin et al., 2003; Hornbrook et al., 2011). Figure 5 indicates that the CIMS HO_2/OH ratio is approximately equal to the modeled HO_2/OH ratio for NO less than 1 ppbv, but surpasses modeled HO_2/OH for NO greater than 1 ppbv, declining less rapidly than models for increasing NO mixing ratios. As the C-130 aircraft and continuous ground-based inorganic and organic species mixing ratios in Golden are similar, this result indicates a disagreement In previous studies, the agreement between measured and modeled HO_x at high NO. While previous studies have shown that measured and modeled OH at high NO are in rough agreement, differences in HO_2 were more severe (Shirley et al., 2006; Kanaya et al., 2007; Dusanter et al., 2009; Sheehy et al., 2010).

Figure 5 indicates $P(O_3)$ as a function of NO levels and time of day. Similar to Cazorla et al. (2012), both measured and modeled diel $P(O_3)$ increased between 0600-0800 LT during morning rush hour, peaked before 1200 LT, and then decreased later in the day with decreasing NO and VOC radical abundances. Occasional, secondary $P(O_3)$ peaks were exhibited between 1400-1600 LT in both OH has been independent of NO, so that the deviation between the measured and modeled $P(O_3)$, likely due to advection of O_3 precursors from the Denver region or increased local traffic emissions. Measured and modeled $P(O_3)$ dependency on NO will typically follow $P(HO_x)$ curves. Since the models were constrained by observed

~~VOCs and NO_x , higher measured than modeled HO_2/OH ratio is due to deviations between measured and modeled HO_2 (Shirley et al., 2006; Kanaya et al., 2007; Dusanter et al., 2009; Sheehy et al., 2010; Ren et al., 2013; Czader et al., 2013; Brune et al., 2014). Modeled RO_2 relative to the CIMS observed RO_2 is also underestimated at high NO was evident as MOPS $\text{P}(\text{O}_3)$ peaked for NO between 3–6 ppbv and modeled $\text{P}(\text{O}_3)$ peaked for NO close to 1 ppbv. This result is presumably for the same atmospheric $\text{P}(\text{HO}_x)$ regimes. If the MOPS accurately portrays net $\text{P}(\text{O}_3)$ behavior, these observations suggest that chemical mechanisms may not be simulating modeled HO_x - NO_x cycling correctly. Thus, models may require further re-examination of the HO_x - NO_x rate coefficients mentioned above, or identification of possible missing reactions involving these two species groups (Fig. 5). Because the C-130 aircraft and ground-based inorganic and organic species mixing ratios in Golden are within 30% on average, a disagreement between measured and modeled peroxy radicals at high NO observed on the aircraft is relevant to understanding the MOPS measurements made at the Golden ground-based site.~~

3.3.4 Mechanism HO_x - NO_x chemistry

~~The missing modeled $\text{P}(\text{O}_3)$ between 0900–1200 LT appears to be approximately linear with NO. A missing HO_x . A hypothesis is that a missing HO_2 or RO_2 source linearly scalable to NO that was not included in the models is plausible. However, 42 forty-two total C_2 - C_{10} VOCs were measured by whole-air canister samples, representing a large suite of organic chemical species within the models, including ones with high OH reactivities that are particularly important for O_3 formation. Therefore, both of the model chemical mechanisms incorporate the dependence of VOC reactivity on NO.~~

~~Measurements of VOC reactivity. Although measurements of VOC reactivity were not available during the field campaign time period and thus are unavailable for comparison to modeled VOC reactivity. However, if a VOC HO_x , the suite of VOCs measured in Golden should sufficiently capture the average VOC reactivity dependence on NO in the mechanisms used here.~~

~~If a VOC source co-emitted with NO_x is missing in the models, it would have to provide an additional HO_2 source of approximately 3×10^7 radicals $\text{cm}^{-3} \text{s}^{-1}$, derived from the average difference between median diel modeled and measured $\text{P}(\text{O}_3)$. Such a missing-VOC source was investigated by adding a) an additional RO_2 source proportional to NO_x , and also b) a generic reaction involving RO_2 and NO to form $\text{HO}_2 + \text{NO}_2 + \text{RO}$ in the MCMv331 using a bimolecular rate coefficient of $8 \times 10^{-12} \text{cm}^3 \text{molec}^{-1} \text{s}^{-1}$. In both cases, since the reaction between the methylperoxy radical (CH_3O_2) and NO is the dominant organic peroxy radical reacting with NO to form new O_3 in both chemical mechanisms, this chemical species was used as a proxy for RO_2 in the following case studies.~~

~~Adding this $\text{RO}_2 + \text{NO}$ reaction to form HO_2 and NO_2 in the MCMv331 only elevates modeled $\text{P}(\text{O}_3)$ throughout the day, and does not alter the diurnal $\text{P}(\text{O}_3)$ pattern (Fig. 6). Adding RO_2 in the MCMv331 proportional to NO_x improves model-measurement $\text{P}(\text{O}_3)$ agreement in the morning, but underestimates the MOPS afternoon $\text{P}(\text{O}_3)$ signal by a factor of two. The model-measurement RO_2 agreement is improved with this case study, yet HO_2/OH is still underestimated relative to measurements for high NO (Fig. 5) suggesting that a missing HO_x source still remains.~~

~~Similarly, a VOC source that could explain prior model-measurement HO_x disagreement has not identified in this study, nor has one been identified in other environments literature studies where missing HO_2 was of similar magnitude to this study, even when proposed missing-VOCs were added to model base case scenarios (Martinez et al., 2003; Kanaya et al., 2007; Dusanter~~

et al., 2009). Further, Brune et al. (2015) discuss that, if this missing HO_x source is also a missing OH loss, then this loss would be evidenced in measurements of OH reactivity at high NO, yet no such OH loss was observed.

5 Peroxynitric acid (HO₂NO₂), which is tied to HO_x and NO_x, is also elevated compared to models at high NO or NO_x (Spencer et al., 2009). Peroxynitric acid thermally decomposes to form HO₂ and NO₂, and can also be weakly photolyzed to form HO₂. Kanaya et al. (2007) propose that increasing the thermal decomposition rate of HO₂NO₂ could resolve model underestimation of HO₂ at high NO, but even when this decomposition rate was increased by a factor of five, it did not correct for higher measured than modeled P(O₃) at high NO. Model sensitivity runs for Golden, CO using this increased decomposition rate for HO₂NO₂ in MCMv331 corroborate this same result (Fig. S26).

10 One reaction proposed in Brune et al. (2015) that may be able to explain observed-to-modeled P(O

3.3.4 Modeled ambient HONO sources

Another hypothesis is that ambient HONO is missing from the model. The production and subsequent photolysis of nitrous acid (HONO) is an important morning HO_x source at high NO or NO_x, often comparable to or larger than other HO_x sources such as peroxide and organic VOC photolysis or O₃ photolysis followed by the subsequent reaction between O(¹D) and water vapor to produce OH. In previous field studies, HONO photolysis was a substantial contributor to daytime HO_x production, but can be largely underpredicted by models, especially in urban environments and may be a more viable solution to the model-measurement discrepancy found in this study.

15 OH+Nitrous acid was not measured during DISCOVER-AQ or FRAPPÉ, but was predicted by the gas-phase RACM2 and MCMv331 based on continuous, ground-based NO_x observations. Model HONO sources in this study only include those in the gas phase. Photolytic conversion of NO+O₂→HO₂+NO₂.

20 Many studies have determined that the reaction between OH and NO to form HONO proceeds at a rate of about $4 \times 10^{-11} \text{ cm}^3 \text{ molec}^{-1} \text{ s}^{-1}$ (Sander et al. (2011) and references therein). have shown that it is possible for molecular oxygen (O₂) to react with vibrationally-excited HONO to form HO₂ and NO₂. However, this reaction would have to proceed with a much slower rate than $4 \times 10^{-11} \text{ cm}^3 \text{ molec}^{-1} \text{ s}^{-1}$ and is only a minor pathway to formation of HO₂ and NO₂. have found that O₂ can react with 25% of excited-state adducts in the OH+acetylene reaction before vibrational quantum state relaxation. In other studies, the formation of the hydrotrioxyl radical (HO₃) on aerosol surfaces (Kleffmann et al., 1998; Arens et al., 2001; Monge et al., 2010); adsorption of HNO₃ was also found to react with O₂, but due to the low-calculated HO₃ abundance in the troposphere, this radical may also be a minor pathway to HO₂. Although the reaction HO₃+NO to form HO₂+NO₂ is exothermic, it, to our knowledge, has not been tested (Murray et al., 2008; Le Picard et al., 2010; Burgess Jr, 2016) on ground surfaces and subsequent photolysis (Zhou et al., 2003, 2011) and other photolytic heterogeneous sources are not included. Therefore, the role of model under-prediction of HONO mixing ratios in the morning can be one cause for modeled versus measured HO₂ reactions with excited-state intermediates to form HO/OH disagreement.

30 Lee et al. (2016) indicate that, even after additional gas-phase and heterogeneous HONO sources were added to MCMv331, HONO was still underestimated relative to models on average, and that a missing HONO source was correlated with J_{NO₂}.

~~NO₂ in the presence of NO remains an open question. We explore the possibility of such a reaction between OH, NO, and O₂ and the product of NO₂ and OH reactivity for an urban area. Furthermore, only model results using measured HONO were able to replicate observed OH levels (Lee et al., 2016). Field studies in which HONO was continuously measured and used to constrain both zero-dimensional and three-dimensional chemical models have been able to replicate observed OH within uncertainty levels, but still exhibit the same behavior of higher measured-than-modeled HO₂ to OH ratios and P(O₃) at high NO (Ren et al., 2003; Martinez et al., 2003; Dusanter et al., 2009; Chen et al., 2010; Czader et al., 2013; Ren et al., 2013; Brune et al., 2015).~~

~~The OH + NO(+O₂) reaction above has been. A HONO source proportional to NO_x was added to the MCMv331 assuming constant atmospheric O₂ levels and varying an effective bimolecular reaction rate between (3-15) × 10⁻¹¹ cm³ molecule⁻¹ s⁻¹. The modeled HO₂/OH dependence on NO closely matches those observed in Fig. 5 when a rate between (9-15) × 10⁻¹¹ cm³ molecule⁻¹ s⁻¹ is used. Further, with this modified chemical mechanism, modeled, resulting in average HONO levels of 0.5-0.9 ppbv between 0700 and 1200 LT, with peak HONO levels of 0.9 ppbv at 1000 LT when MOPS P(O₃) approaches median-observed exhibits its diel peak. This case study approximately replicates the observed morning P(O₃) with a maximum rate between 1000-1200 LT reaching 10 ppbv h⁻¹ (Fig. S2). The modeled diurnal curve then decreases later in the day similar to the median-6) and observed OH within uncertainty levels. However, while added HONO in the MCMv331 improves the agreement between observed and modeled diel P(O₃) diel curve presented in Fig. 2. The improved agreement between measured and modeled, mid-morning HONO levels needed to do so are over a factor of two higher than those observed in other areas within Colorado (Brown et al., 2013; VandenBoer et al., 2013) and in environments with much higher NO_x levels (VandenBoer et al., 2015). Thus, the HO₂/OH and ratio and the abnormally high HONO required to match the observed P(O₃) behavior suggests that this reaction scheme is worth examining in more detail.~~

3.3.5 Reactive chlorine chemistry

~~Other hypotheses for model underestimation of provide evidence that at most only a part of the observed P(O₃) relative to observations at high NO were explored, including the impacts of the can be explained by atmospheric HONO.~~

3.3.5 Reactive chlorine chemistry

~~Model under-representation of nitryl chloride (ClNO₂) production in current chemical mechanisms is another possible cause of the model underestimation of P(O₃). Nitryl chloride serves as a nocturnal NO_x reservoir and, when photolyzed, can produce additional reactive chlorine (Cl) and nitrogen dioxide (NO₂). Reactive chlorine, even at low mixing ratios, has been found to serve as a major oxidant for VOCs, possibly increasing HO₂ and O₃ production in the early morning hours by as much as 30% (Finlayson-Pitts et al., 1989; Atkinson et al., 1999; Chang et al., 2002; Osthoff et al., 2008). The effects of ClNO₂ production on chlorine chemistry and VOC oxidation have been provided in the literature as one possible explanation for measured versus modeled model-data HO₂ differences mismatch at higher NO levels (Thornton et al., 2010; Riedel et al., 2014; Xue et al., 2015).~~

Heterogeneous uptake of dinitrogen pentoxide (N₂O₅) on chloride-containing aerosol particles can produce nitric acid (HNO₃) and ClNO₂ in both marine and continental environments through the following reaction:



where k_{het} is the heterogeneous reaction rate coefficient dependent upon the aerosol surface area density and the N_2O_5 uptake coefficient on chloride-containing aerosols, and ϕ is the ClNO_2 product yield.

To test this hypothesis, we constrained the MCMv331 with continuous, cavity ring-down spectroscopy measurements of N_2O_5 (Brown et al., 2002) from a nearby measurement site (Boulder Atmospheric Observatory; 40.050°N, 105.010°W), and
 10 implemented a reduced chlorine chemical mechanism in the MCMv331 provided by Riedel et al. (2014). We assumed an N_2O_5 uptake coefficient of 0.02, which is within the range of coefficients calculated in prior field studies (Wagner et al., 2013; Riedel et al., 2013) and laboratory experiments (Zetzsch and Behnke, 1992; Behnke et al., 1997). To be consistent with previous studies near Golden, the aerosol surface area density was varied between 150 and 250 $\mu\text{m}^2 \text{cm}^{-3}$, and ϕ is varied
 15 with relative humidity and aerosol surface area and composition (Thornton and Abbatt, 2005; Bertram and Thornton, 2009; Roberts et al., 2009; Thornton et al., 2010; Wagner et al., 2013; Riedel et al., 2013), but modeling over a range of values can provide a qualitative prediction of ClNO_2 production effects on model $\text{P}(\text{O}_3)$ in this region. In each model case, the ~~MCMv331~~
~~MCMv331~~ runs including ClNO_2 production and Cl-VOC chemistry resulted in average ClNO_2 mixing ratios between 0.04 and 0.13 ppbv during the early morning hours (0300-0600 LT) and a slight increase in diurnal $\text{P}(\text{O}_3)$ values of less than 5%.
 20 Thus, although chlorine chemistry can have a large effect on $\text{P}(\text{O}_3)$ during the winter and for marine environments, these model runs indicate that Cl chemistry does not play a large enough role in O_3 photochemistry during this summer campaign to explain the morning observed discrepancy between measured and modeled O_3 formation rates in Golden, CO.

3.3.6 Nitrous acid photolysis

~~Perhaps more of an important HO_x source in the morning hours at high NO or NO_x than ClNO_2 is the production and photolysis
 25 of HONO. Other important HO_x sources include hydrogen peroxide and organic VOC photolysis, and O_3 photolysis followed by the subsequent reaction between $\text{O}(^1\text{D})$ and water vapor to produce OH. In previous field studies, HONO photolysis contributed largely to the daytime HO_x production (Alicke et al., 2003; Ren et al., 2003; Kanaya et al., 2007; Dusanter et al., 2009; Volkan~~

~~Nitrous acid was not measured during DISCOVER-AQ or FRAPP, and was thus predicted by the RACM2 and MCMv331
 30 based on continuous, ground-based NO_x observations. Therefore, model under-prediction of HONO mixing ratios in the morning can be one cause for modeled versus measured HO_2/OH disagreement. However, studies in which HONO was continuously measured and used to constrain both zero-dimensional and three-dimensional chemical models still exhibited the same behavior of higher measured than modeled HO_2 to OH ratios at high NO (Ren et al., 2003; Martinez et al., 2003; Dusanter et al., 2009). Thus, this morning HO_x source is likely not the sole cause for model under-prediction of model HO_2 —and thus, $\text{P}(\text{O}_3)$ —at high NO_x found here and in previous studies.~~

3.4 Implications for O₃ mitigation strategies

3.4.1 NO_x-VOC sensitivity

5 The underestimation of model P(O₃) relative to the MOPS at high NO or NO_x can have far-reaching implications for model assessment of the dependency of P(O₃) on NO_x and VOCs. When examining model sensitivity to NO_x, levels were adjusted up or down by a factor of two and as a result, increasing NO_x levels decreases P(O₃) (as in a VOC-sensitive regime) while lowering NO_x levels acts to increase P(O₃) (Fig. 6).

The fraction of free radicals removed by NO_x, L_N/Q , has been used in the literature to assess NO_x-VOC sensitivity in
10 regions experiencing high O₃ (Daum et al., 2004; Kleinman, 2005; Ren et al., 2013). Here, L_N is the rate of total free radical removal by NO_x, and Q is the total radical production rate. When significantly above 0.5, the atmosphere is within a VOC-sensitive regime, while when significantly below 0.5, the atmosphere is within a NO_x-sensitive regime (Kleinman, 2005). The median L_N/Q was calculated with the RACM2 using full-campaign observations, indicating that Golden-the Golden, CO modeled P(O₃) is VOC-sensitive before 1200 LT and NO_x-sensitive thereafter according to models (Fig. S3S4). During
15 DISCOVER-AQ and FRAPPÉ, model sensitivity studies conducted for the Boulder Atmospheric Observatory site just north-east of Golden also found maximum photochemical O₃ to be largely NO_x-sensitive in the afternoon (McDuffie et al., 2016). However, if HO₂ is underestimated by chemical mechanisms such as the RACM2 and the MCMv3.3.1, relative to observations for NO levels greater than a few ppbv, then the total radical production rate, Q , may also be underestimated, thereby shifting the NO_x-VOC sensitivity more towards a L_N/Q towards NO_x-sensitive regime. Model runs including
20 the proposed OH + NO reaction indicate a shift from VOC- to NO_x-sensitive conditions approximately one to two hours earlier in the morning than base-case model chemistry (Fig. S3). sensitivity in the early morning and prolonging this regime during times of the day when O₃ production is largest.

The largest O₃ formation rates are measured before 1200 between 0900-1100 LT when NO_x and VOC emissions are high and the mixing layer is relatively shallow depth is relatively developed at 600 to 1000 m on average. Although a shallow mixing
25 layer is shallower mixing layer could be one reason for high MOPS P(O₃) during the morning hours before 1100 LT, we note that secondary diurnal MOPS P(O₃) peaks are also evidenced on individual days alongside increased NO_x and VOCs during afternoon rush hour in a deeper fully-developed mixing layer. Further, high P(O₃) and the shift from VOC- to NO_x-sensitive O₃ formation-sensitivity in the late morning could be attributed to early-morning entrainment of VOCs from the free troposphere in the absence of NO_x entrainment. However, these VOCs in the upper troposphere are longer-lived and are less important in
30 propagating O₃ formation than other, higher reactivity VOCs. Therefore, although entrainment of species during the morning hours and the depth of the mixing layer influence NO_x-VOC sensitivity and these high morning P(O₃) rates, it is more likely that O₃ precursor species at the surface level predominantly influence observed are the predominant factors influencing P(O₃) for this study.

Generally speaking, while Although longer-term analyses are generally required to suggest effective O₃ reduction strategies for Golden and surrounding regions, if the P(O₃) NO_x-VOC sensitivity is shifted more towards a NO_x-sensitive regime

in the morning as the MOPS observations suggest, reducing NO_x ~~may would~~ be an effective strategy for O_3 mitigation in the ~~Colorado Front Range~~ Golden, CO and its immediate surroundings.

5 3.4.2 O_x advection

Ozone formation precursors can be transported westward to Golden because of the Colorado Front Range terrain and its induced wind patterns. When air in Golden is influenced by O_3 precursor emissions from the east (e.g. the Denver metropolitan and Commerce City regions), greater anthropogenic VOC and NO mixing ratios are measured on average. Thus, we evaluate calculated O_3 advection using Eq. (1) in an attempt to evaluate the impact of O_3 advection derived from the MOPS and the
10 models on observed O_3 patterns in Golden.

Measured O_x maxima are 2-7 ppbv greater on these “plume” days than when air is advected from elsewhere, and higher $\text{P}(\text{O}_3)$ is measured by the MOPS than is modeled by the RACM2 and MCMv331 (Fig. 7). This result is roughly consistent with the difference between measured and modeled $\text{P}(\text{O}_3)$ as a function of NO shown in Fig. 4. When winds are not easterly (“non-plume” days), lower levels of anthropogenic VOCs ~~and~~ NO , and lower O_x maxima are observed, ~~and average~~. Average
15 measured diel $\text{P}(\text{O}_3)$ is ~~45~~ also 20% lower than on plume days. ~~This~~ The MOPS behavior stands in contrast to the models, where average diel RACM2 and MCMv331 $\text{P}(\text{O}_3)$ is approximately 30% ~~lower on plume days than all other days~~. higher on non-plume days than on plume days.

A simple advection analysis was performed to determine the factors in Eq. (1) that most ~~likely~~ contribute to observed O_x levels in Fig. 7 for ~~plume and non-plume days~~ the campaign period. The transport rate of O_x out of the mixing layer
20 through deposition is calculated to be at most 1 ppbv h^{-1} and is neglected here. The morning O_3 entrainment rate during DISCOVER-AQ and ~~FRAPPE~~ FRAPPÈ has been calculated for the Colorado Front Range region to be 5 ppbv h^{-1} on average, with afternoon average entrainment rates of approximately -1 ppbv h^{-1} (Kaser et al. (2016), *in prep*). Assuming an average entrainment rate of 5 ppbv h^{-1} for morning hours between 0600-1200 LT and an O_x entrainment rate of -1 ppbv h^{-1} for times between 1200-1800 LT and subtracting diel entrainment and observed $\text{P}(\text{O}_x)$ from the local diel O_x rate of change, the average
25 O_x advection rate derived from MOPS and models between 0600-1800 LT is ~~-5.1 and -5.4 to~~ -2.4 ppbv h^{-1} on plume days, and ~~-1.7 and to~~ -3.5 ppbv h^{-1} for all other days, respectively. This quick calculation suggests that advection contributes weakly to observed O_x , while either entrainment or $\text{P}(\text{O}_x)$ dominate the O_x patterns observed in Golden and ~~likely~~ its surrounding areas. Because these advection rates are derived quantities from the MOPS and the models, and both methods for determining $\text{P}(\text{O}_x)$ contain ~~relatively high~~ substantial uncertainty, it is difficult to quantitatively assess O_x advection rates in Golden, CO ~~as these~~
30 ~~errors propagate to advection rate uncertainties of up to a factor of two~~. Decreasing the uncertainty in $\text{P}(\text{O}_x)$ is thus salient for accurately calculating the terms in Eq. (1) contributing to observed O_x levels in the Colorado Front Range.

4 Conclusions

Comparisons were made between $\text{P}(\text{O}_3)$ measured ~~in-situ~~ in situ by a second-generation Penn State MOPS ~~and~~ photochemical box modeled $\text{P}(\text{O}_3)$ using both lumped and near-explicit chemical mechanisms. These ~~2014 comparisons during~~ comparisons

during the 2014 DISCOVER-AQ and FRAPPÉ field campaigns in the Colorado Front Range show that modeled median diel modeled $P(O_3)$ is underestimated relative to the MOPS by roughly a factor of two. This underestimation is most pronounced between 0900 and 1200 LT during peak O_3 production hours when high levels in mid-morning, when actinic flux is increasing and morning rush hour abundances of NO_x and VOCs are present due to rush hour emissions.

5 This result is not completely explained by several different possibilities: decreasing. This result corroborates to previous studies that had $P(O_3)$ measured by MOPSS (Cazorla et al., 2012; Baier et al., 2015). Thus, this model-data $P(O_3)$ mismatch appears to come from unknowns in the chamber or atmospheric chemistry and not from one particular environment.

The uncertainties in both the measurement and the model are substantial. The measurement uncertainty is about ± 5 ppbv h^{-1} , with the largest portion due to the zeroing of the daily negative drifting of the differential O_3 measurement. Model $P(O_3)$ uncertainty is large about 30% (1σ confidence) during peak $P(O_3)$ hours; factors influencing this uncertainty during the day include uncertainty such as uncertainty in the kinetic rate coefficients of HO_x - NO_x cycling reactions are most significant. Despite these uncertainties, the difference between the diel behavior and values of measured and modeled $P(O_3)$ is significant.

Upon further analysis of the discrepancy between measured and modeled $P(O_3)$ at high NO_x , it was found that the measured HO_2 -peroxy radical behavior as a function of NO was similar to studies previously reported in the literature in which. In these studies, the measured HO_2 to OH ratio decreases/OH ratio and measured RO_2 decrease less rapidly than modeled ratios that modeled for higher NO levels, most likely causing causing measured or calculated $P(O_3)$ measured by the MOPS to be up to 2-3 times to be several factors larger than modeled $P(O_3)$ between 0900 and 1200 LT. As such, neither MOPS chamber chemistry artifacts, reactive chlorine chemistry, nor model sensitivity studies case studies that add additional peroxy radical sources can fully explain this disagreement between modeled and measured model-data $P(O_3)$. If we include a reaction of $OH + NO$ to form HO_2 and NO_2 with a bimolecular reaction rate coefficient of $(9-15) \times 10^{-11} \text{ cm}^3 \text{ molec}^{-1} \text{ s}^{-1}$, the model can replicate the MOPS observed mismatch. While an additional HONO source proportional to NO_x can help to improve diel $P(O_3)$ patterns, mid-morning HONO levels needed to approximate MOPS $P(O_3)$ behavior in this Golden, CO study are at least a factor of two higher than HONO levels observed in other environments, including ones nearby in Colorado. Additional RO_2 sources can approximate $P(O_3)$ morning diurnal patterns, but underestimate $P(O_3)$ in the afternoon relative to the MOPS by roughly a factor of two. Neither peroxy radical addition mechanism can approximate the behavior of HO_x radicals as a function of NO relative to measurements.

More research must be conducted on both fronts to understand the differences between modeled and measured $P(O_3)$. The second-generation MOPS is still in early stages of development and much more time and more rigorous testing is needed to decrease the MOPS absolute measurement offset uncertainty through the reduction of O_3 analyzer drifting. On the other hand and improvement in the precision of this analyzer. Conversely, model comparisons highlight the need to revisit current mechanism reaction rate coefficients and product yields involving HO_x - NO_x cycling, and to investigate possible missing HO_x sources chemistry, including possible missing peroxy radical chemistry at high NO_x levels.

If models are truly under-predicting HO_2 in the early morning, the MOPS accurately predicts morning $P(O_3)$, then L_N/Q metrics from observation-constrained models that calculate radical mixing ratios may be incorrectly assessing NO_x or VOC

O₃ production sensitivity and the efficacy of O₃ reduction strategies. ~~Further, the~~ The use of these mechanisms in CTMs ~~can~~
10 ~~could~~ create significant differences between modeled and observed P(O₃) during peak O₃ production hours ~~and can translate~~
~~to large discrepancies~~. Further, the plethora of chemical mechanisms available for use in these models create a large spread
in model O₃ predictions. Thus, differences between measured and modeled P(O₃) can have substantial and potentially costly
implications for O₃ mitigation strategies that are put in place in O₃ NAAQS non-attainment areas. The MOPS measurements
indicate that P(O₃) in Golden, CO and its surrounding areas ~~are is~~ more NO_x-sensitive ~~in the early morning than models~~
15 ~~currently predict in the morning hours~~, suggesting that NO_x emission reductions in this region ~~are could be~~ a viable solution
for O₃ mitigation ~~in the Colorado Front Range~~.

5 Data availability

The MCM version 3.3.1 is freely available at <http://mcm.leeds.ac.uk/MCM/> and the University of Washington Chemical Model
(UWCM) framework used to run MCMv331 is available to the public from G. Wolfe. Meteorological and chemical data
20 collected during the DISCOVER-AQ and FRAPPÈ studies are available at [http://www-air.larc.nasa.gov/missions/discover-](http://www-air.larc.nasa.gov/missions/discover-aq/discover-aq.html)
[aq/discover-aq.html](https://www2.acom.ucar.edu/frappe) and <https://www2.acom.ucar.edu/frappe>.

Author S. Brown serves on the editorial board of this journal. No other authors declare any conflicts of interest.

Acknowledgements. We gratefully acknowledge the entire DISCOVER-AQ and FRAPPÈ teams for the collection of ground and airborne
25 measurement data in this work. We kindly acknowledge R. Cohen for the provision of data used in these model studies. PTR-ToF-MS
measurements during DISCOVER-AQ were carried out by P. Eichler, T. Mikoviny, and M. Müller, and were supported by the Austrian
Federal Ministry for Transport, Innovation and Technology (bmvit) through the Austrian Space Applications Programme (ASAP) of the
Austrian Research Promotion Agency (FFG). We thank G. Wolfe for provision of and help with the MCM model framework, W. Goliff for
the provision of the RACM2, and J. Thornton for thoughtful discussions. We thank the two anonymous reviewers for their useful comments.
30 For the use of the web version of the HYSPLIT model (<http://www.ready.noaa.gov>), we acknowledge the NOAA Air Resources Laboratory.
This work was funded by NASA grants NNX14AR83G and NNX12AB84G.

References

- Alicke, B., Geyer, A., Hofzumahaus, A., Holland, F., Konrad, S., Pätz, H., Schäfer, J., Stutz, J., Volz-Thomas, A., and Platt, U.: OH formation by HONO photolysis during the BERLIOZ experiment, *Journal of Geophysical Research: Atmospheres*, 108, 2003.
- 35 Apel, E., Hills, A., Lueb, R., Zindel, S., Eisele, S., and Riemer, D.: A fast-GC/MS system to measure C2 to C4 carbonyls and methanol aboard aircraft, *Journal of Geophysical Research: Atmospheres*, 108, 2003.
- Appel, K. W., Gilliland, A. B., Sarwar, G., and Gilliam, R. C.: Evaluation of the Community Multiscale Air Quality (CMAQ) model version 4.5: Sensitivities impacting model performance: Part I: Ozone, *Atmospheric Environment*, 41, 9603–9615, doi:10.1016/j.atmosenv.2007.08.044, <http://www.sciencedirect.com/science/article/pii/S1352231007007534>, 2007.
- Arens, F., Gutzwiller, L., Baltensperger, U., Gäggeler, H. W., and Ammann, M.: Heterogeneous reaction of NO₂ on diesel soot particles, *Environmental science & technology*, 35, 2191–2199, 2001.
- 5 Atkinson, R., Baulch, D., Cox, R., Hampson Jr, R., Kerr, J., Rossi, M., and Troe, J.: Evaluated kinetic and photochemical data for atmospheric chemistry, organic species: Supplement VII, *Journal of Physical and chemical reference Data*, 28, 191–393, 1999.
- Baier, B. C., Brune, W. H., Lefer, B. L., Miller, D. O., and Martins, D. K.: Direct ozone production rate measurements and their use in assessing ozone source and receptor regions for Houston in 2013, *Atmospheric Environment*, 114, 83–91, doi:10.1016/j.atmosenv.2015.05.033, <http://www.sciencedirect.com/science/article/pii/S1352231015301060>, 2015.
- 10 Banta, R. M.: Daytime Boundary-Layer Evolution over Mountainous Terrain. Part I: Observations of the Dry Circulations, *Mon. Wea. Rev.*, 112, 340–356, doi:10.1175/1520-0493(1984)112<0340:DBLEOM>2.0.CO;2, [http://journals.ametsoc.org/doi/abs/10.1175/1520-0493\(1984\)112%3C0340%3ADBLEOM%3E2.0.CO%3B2](http://journals.ametsoc.org/doi/abs/10.1175/1520-0493(1984)112%3C0340%3ADBLEOM%3E2.0.CO%3B2), 1984.
- Behnke, W., George, C., Scheer, V., and Zetzsch, C.: Production and decay of ClNO₂ from the reaction of gaseous N₂O₅ with NaCl solution: Bulk and aerosol experiments, *J. Geophys. Res.*, 102, 3795–3804, doi:10.1029/96JD03057, <http://onlinelibrary.wiley.com/doi/10.1029/96JD03057/abstract>, 1997.
- 15 Bell, M. L., McDermott, A., Zeger, S., Samet, J., and Dominici, F.: Ozone and Short-term Mortality in 95 US Urban Communities 1987-2000, *Journal of the American Medical Association*, 292, doi:10.1001/jama.292.19.2372, 2004.
- Bertram, T. H. and Thornton, J. A.: Toward a general parameterization of N₂O₅ reactivity on aqueous particles: the competing effects of particle liquid water, nitrate and chloride, *Atmos. Chem. Phys.*, 9, 8351–8363, doi:10.5194/acp-9-8351-2009, <http://www.atmos-chem-phys.net/9/8351/2009/>, 2009.
- 20 Bloss, C., Wagner, V., Jenkin, M. E., Volkamer, R., Bloss, W. J., Lee, J. D., Heard, D. E., Wirtz, K., Martin-Reviejo, M., Rea, G., Wenger, J. C., and Pilling, M. J.: Development of a detailed chemical mechanism (MCMv3.1) for the atmospheric oxidation of aromatic hydrocarbons, *Atmospheric Chemistry and Physics*, 5, 641–664, doi:10.5194/acp-5-641-2005, <http://www.atmos-chem-phys.net/5/641/2005/>, 2005.
- Brown, S. S., Stark, H., Ciciora, S. J., McLaughlin, R. J., and Ravishankara, A.: Simultaneous in situ detection of atmospheric NO₃ and N₂O₅ via cavity ring-down spectroscopy, *Review of scientific instruments*, 73, 3291–3301, 2002.
- 25 Brown, S. S., Thornton, J. A., Keene, W. C., Pszenny, A. A., Sive, B. C., Dube, W. P., Wagner, N. L., Young, C. J., Riedel, T. P., Roberts, J. M., et al.: Nitrogen, Aerosol Composition, and Halogens on a Tall Tower (NACHTT): Overview of a wintertime air chemistry field study in the front range urban corridor of Colorado, *Journal of Geophysical Research: Atmospheres*, 118, 8067–8085, 2013.
- Brune, W. H., Baier, B. C., Thomas, J., Ren, X., Cohen, R., Pusede, S. E., Browne, E., Goldstein, A., Gentner, D. R., Keutsch, F. N., Thornton, J. A., Harrold, S., Lopez-Hilfiker, F., and Wennberg, P. O.: Ozone Production Chemistry in the Presence of Urban Plumes, *Faraday Discuss.*, doi:10.1039/C5FD00204D, <http://pubs.rsc.org/en/content/articlelanding/2015/fd/c5fd00204d>, 2015.
- 30

- Burgess Jr, D. R.: An Evaluation of Gas Phase Enthalpies of Formation for Hydrogen-Oxygen (HO_xO_y) Species, *Journal of Research of the National Institute of Standards and Technology*, 121, 108, 2016.
- Calvert, J. G., Orlando, J. J., Stockwell, W. R., and Wallington, T. J.: The Mechanisms of Reactions Influencing Atmospheric Ozone, Oxford University Press, 2015.
- Cantrell, C. A., Edwards, G., Stephens, S., Mauldin, R., Zondlo, M., Kosciuch, E., Eisele, F., Shetter, R., Lefer, B., Hall, S., et al.: Peroxy radical behavior during the Transport and Chemical Evolution over the Pacific (TRACE-P) campaign as measured aboard the NASA P-3B aircraft, *Journal of Geophysical Research: Atmospheres*, 108, 2003.
- 35 Cazorla, M. and Brune, W. H.: Measurement of Ozone Production Sensor, *Atmospheric Measurement Techniques*, 3, 545–555, doi:10.5194/amt-3-545-2010, 2010.
- Cazorla, M., Brune, W. H., Ren, X., and Lefer, B.: Direct measurement of ozone production rates in Houston in 2009 and comparison with two estimation methods, *Atmos. Chem. Phys.*, 12, 1203–1212, doi:10.5194/acp-12-1203-2012, 2012.
- 5 Chang, S., McDonald-Buller, E., Kimura, Y., Yarwood, G., Neece, J., Russell, M., Tanaka, P., and Allen, D.: Sensitivity of urban ozone formation to chlorine emission estimates, *Atmospheric Environment*, 36, 4991–5003, 2002.
- Chen, S. and Brune, W. H.: Global sensitivity analysis of ozone production and O₃-NO_x-VOC limitation based on field data, *Atmospheric Environment*, 55, 288–296, doi:10.1016/j.atmosenv.2012.03.061, 2012.
- Chen, S., Ren, X., Mao, J., Chen, Z., Brune, W. H., Lefer, B., Rappenglück, B., Flynn, J., Olson, J., and Crawford, J. H.: A comparison of chemical mechanisms based on TRAMP-2006 field data, *Atmospheric Environment*, 44, 4116–4125, doi:10.1016/j.atmosenv.2009.05.027, 10 2010.
- Chen, S., Brune, W. H., Oluwole, O. O., Kolb, C. E., Bacon, F., Li, G., and Rabitz, H.: Global sensitivity analysis of the regional atmospheric chemical mechanism: an application of random sampling-high dimensional model representation to urban oxidation chemistry, *Environmental science & technology*, 46, 11 162–11 170, doi:10.1021/es301565w, PMID: 22963531, 2012.
- 15 Colman, J. J., Swanson, A. L., Meinardi, S., Sive, B. C., Blake, D. R., and Rowland, F. S.: Description of the analysis of a wide range of volatile organic compounds in whole air samples collected during PEM-Tropics A and B, *Analytical Chemistry*, 73, 3723–3731, 2001.
- Crilley, L., Kramer, L., Pope, F. D., Whalley, L. K., Cryer, D. R., Heard, D. E., Lee, J., Reed, C., and Bloss, W.: On the interpretation of in situ HONO observations via photochemical steady state, *Faraday Discussions*, 2016.
- Czader, B. H., Li, X., and Rappenglueck, B.: CMAQ modeling and analysis of radicals, radical precursors, and chemical transformations, *J. Geophys. Res. Atmos.*, 118, 11,376–11,387, doi:10.1002/jgrd.50807, <http://onlinelibrary.wiley.com/doi/10.1002/jgrd.50807/abstract>, 20 2013.
- Daum, P. H., Kleinman, L. I., Springston, S. R., Nunnermacker, L. J., Lee, Y.-N., Weinstein-Lloyd, J., Zheng, J., and Berkowitz, C. M.: Origin and properties of plumes of high ozone observed during the Texas 2000 Air Quality Study (TexAQS 2000), *J. Geophys. Res.*, 109, D17 306, doi:10.1029/2003JD004311, <http://onlinelibrary.wiley.com/doi/10.1029/2003JD004311/abstract>, 2004.
- 25 Day, D., Wooldridge, P., Dillon, M., Thornton, J., and Cohen, R.: A thermal dissociation laser-induced fluorescence instrument for in situ detection of NO₂, peroxy nitrates, alkyl nitrates, and HNO₃, *Journal of Geophysical Research: Atmospheres*, 107, 2002.
- Dodge, M. C.: Chemical oxidant mechanisms for air quality modeling: critical review, *Atmospheric Environment*, 34, 2103–2130, doi:10.1016/S1352-2310(99)00461-6, <http://www.sciencedirect.com/science/article/pii/S1352231099004616>, 2000.
- Dusanter, S., Vimal, D., Stevens, P., Volkamer, R., and Molina, L.: Measurements of OH and HO₂ concentrations during the MCMA-2006 field campaign–Part 1: Deployment of the Indiana University laser-induced fluorescence instrument, *Atmospheric Chemistry and Physics*, 30 9, 1665–1685, 2009.

- Emmerson, K., Carslaw, N., Carpenter, L., Heard, D., Lee, J., and Pilling, M.: Urban atmospheric chemistry during the PUMA campaign 1: Comparison of modelled OH and HO₂ concentrations with measurements, *Journal of Atmospheric Chemistry*, 52, 143–164, 2005.
- Emmerson, K., Carslaw, N., Carslaw, D., Lee, J., McFiggans, G., Bloss, W., Gravestock, T., Heard, D., Hopkins, J., Ingham, T., Pilling, M. J., Smith, S., Jacob, D. J., and Monks, P. S.: Free radical modelling studies during the UK TORCH Campaign in Summer 2003, 7, 167–181, <http://www.atmos-chem-phys.org/7/167/2007/acp-7-167-2007.pdf>, 2007.
- Faloona, I., Tan, D., Brune, W. H., Jaeglé, L., Jacob, D. J., Kondo, Y., Koike, M., Chatfield, R., Pueschel, R., Ferry, G., Sachse, G., Vay, S., Anderson, B., Hannon, J., and Fuelberg, H.: Observations of HO_x and its relationship with NO_x in the upper troposphere during SONEX, *J. Geophys. Res.*, 105, 3771–3783, doi:10.1029/1999JD900914, <http://onlinelibrary.wiley.com/doi/10.1029/1999JD900914/abstract>, 2000.
- Finlayson-Pitts, B., Wingen, L., Sumner, A., Syomin, D., and Ramazan, K.: The heterogeneous hydrolysis of NO₂ in laboratory systems and in outdoor and indoor atmospheres: An integrated mechanism, *Physical Chemistry Chemical Physics*, 5, 223–242, doi:10.1039/B208564J, 2003.
- 5 Finlayson-Pitts, B. J. and Pitts, J. N.: The chemical basis of air quality- Kinetics and mechanisms of photochemical air pollution and application to control strategies, *Advances in environmental science and technology.*, 7, 75–162, 1977.
- Finlayson-Pitts, B. J., Ezell, M. J., and Pitts, J. N.: Formation of chemically active chlorine compounds by reactions of atmospheric NaCl particles with gaseous N₂O₅ and ClONO₂, *Nature*, 337, 241–244, doi:10.1038/337241a0, <http://www.nature.com/nature/journal/v337/n6204/abs/337241a0.html>, 1989.
- 10 Fuchs, H., Bohn, B., Hofzumahaus, A., Holland, F., Lu, K., Nehr, S., Rohrer, F., and Wahner, A.: Detection of HO₂ by laser-induced fluorescence: calibration and interferences from RO₂ radicals, *Atmospheric Measurement Techniques*, 4, 1209, 2011.
- George, C., Strekowski, R., Kleffmann, J., Stemmler, K., and Ammann, M.: Photoenhanced uptake of gaseous NO₂ on solid organic compounds: a photochemical source of HONO, *Faraday Discussions*, 130, 195–210, 2005.
- Gilliland, A. B., Hogrefe, C., Pinder, R. W., Godowitch, J. M., Foley, K. L., and Rao, S. T.: Dynamic evaluation of regional air quality models: Assessing changes in O₃ stemming from changes in emissions and meteorology, *Atmospheric Environment*, 42, 5110–5123, doi:10.1016/j.atmosenv.2008.02.018, <http://www.sciencedirect.com/science/article/pii/S1352231008001374>, 2008.
- 15 Goliff, W. S., Stockwell, W. R., and Lawson, C. V.: The regional atmospheric chemistry mechanism, version 2, *Atmospheric Environment*, 68, 174–185, doi:10.1016/j.atmosenv.2012.11.038, <http://www.sciencedirect.com/science/article/pii/S1352231012011065>, 2013.
- Griffith, S., Hansen, R., Dusanter, S., Michoud, V., Gilman, J., Kuster, W., Veres, P., Graus, M., Gouw, J., Roberts, J., et al.: Measurements of hydroxyl and hydroperoxy radicals during CalNex-LA: Model comparisons and radical budgets, *Journal of Geophysical Research: Atmospheres*, 121, 4211–4232, 2016.
- 20 Haagen-Smit, A. J., Bradley, C. E., and Fox, M. M.: Ozone Formation in Photochemical Oxidation of Organic Substances, *Ind. Eng. Chem.*, 45, 2086–2089, doi:10.1021/ie50525a044, <http://dx.doi.org/10.1021/ie50525a044>, 1953.
- Hofzumahaus, A., Rohrer, F., Lu, K., Bohn, B., Brauers, T., Chang, C.-C., Fuchs, H., Holland, F., Kita, K., Kondo, Y., Li, X., Lou, S., Shao, M., Zeng, L., Wahner, A., and Zhang, Y.: Amplified Trace Gas Removal in the Troposphere, *Science*, 324, 1702–1704, 2009.
- 25 Hornbrook, R. S., Crawford, J. H., Edwards, G. D., Goyea, O., Mauldin III, R. L., Olson, J. S., and Cantrell, C. A.: Measurements of tropospheric HO₂ and RO₂ by oxygen dilution modulation and chemical ionization mass spectrometry, *Atmos. Meas. Tech.*, 4, 735–756, doi:10.5194/amt-4-735-2011, <http://www.atmos-meas-tech.net/4/735/2011/>, 2011.
- Im, U., Bianconi, R., Solazzo, E., Kioutsioukis, I., Badia, A., Balzarini, A., Baró, R., Bellasio, R., Brunner, D., Chemel, C., et al.: Evaluation of operational on-line-coupled regional air quality models over Europe and North America in the context of AQMEII phase 2. Part I: Ozone, *Atmospheric Environment*, 115, 404–420, 2015.

- Jaegle, L., Jacob, D. J., Brune, W. H., Tan, D., Faloon, I. C., Weinheimer, A. J., Ridley, B. A., Campos, T. L., and Sachse, G. W.: Sources of HO_x and production of ozone in the upper troposphere over the United States, *Geophysical Research Letters*, 25, 1709–1712, doi:10.1029/98GL00041, <http://dx.doi.org/10.1029/98GL00041>, 1998.
- 35 Jeffries, H. E. and Tonnesen, S.: A comparison of two photochemical reaction mechanisms using mass balance and process analysis, *Atmospheric Environment*, 28, 2991–3003, 1994.
- Jenkin, M. E., Saunders, S. M., and Pilling, M. J.: The tropospheric degradation of volatile organic compounds: a protocol for mechanism development, *Atmospheric Environment*, 31, 81–104, doi:10.1016/S1352-2310(96)00105-7, <http://www.sciencedirect.com/science/article/pii/S1352231096001057>, 1997.
- Jenkin, M. E., Saunders, S. M., Wagner, V., and Pilling, M. J.: Protocol for the development of the Master Chemical Mechanism, MCM v3 (Part B): tropospheric degradation of aromatic volatile organic compounds, *Atmos. Chem. Phys.*, 3, 181–193, doi:10.5194/acp-3-181-2003, <http://www.atmos-chem-phys.net/3/181/2003/>, 2003.
- 5 Jenkin, M. E., Young, J. C., and Rickard, A. R.: The MCM v3.3.1 degradation scheme for isoprene, *Atmos. Chem. Phys.*, 15, 11 433–11 459, doi:10.5194/acp-15-11433-2015, <http://www.atmos-chem-phys.net/15/11433/2015/>, 2015.
- Jimenez, P., Baldasano, J. M., and Dabdub, D.: Comparison of photochemical mechanisms for air quality modeling, *Atmospheric Environment*, 37, 4179–4194, doi:10.1016/S1352-2310(03)00567-3, 2003.
- 10 Kanaya, Y., Cao, R., Akimoto, H., Fukuda, M., Komazaki, Y., Yokouchi, Y., Koike, M., Tanimoto, H., Takegawa, N., and Kondo, Y.: Urban photochemistry in central Tokyo: 1. Observed and modeled OH and HO₂ radical concentrations during the winter and summer of 2004, *J. Geophys. Res.*, 112, D21 312, doi:10.1029/2007JD008670, <http://onlinelibrary.wiley.com/doi/10.1029/2007JD008670/abstract>, 2007.
- Kanaya, Y., Fukuda, M., Akimoto, H., Takegawa, N., Komazaki, Y., Yokouchi, Y., Koike, M., and Kondo, Y.: Urban photochemistry in central Tokyo: 2. Rates and regimes of oxidant (O₃+ NO₂) production, *Journal of Geophysical Research: Atmospheres*, 113, 2008.
- 15 Kaser, L., Patton, E., Pfister, G. G., Weinheimer, A., and Coauthors: The effect of vertical mixing on observed and modeled surface ozone in the Colorado Front Range, *in prep*, 2016.
- Kleffmann, J., Becker, K., and Wiesen, P.: Heterogeneous NO₂ conversion processes on acid surfaces: possible atmospheric implications, *Atmospheric Environment*, 32, 2721–2729, 1998.
- 20 Kleinman, L. I.: The dependence of tropospheric ozone production rate on ozone precursors, *Atmospheric Environment*, 39, 575–586, doi:10.1016/j.atmosenv.2004.08.047, 2005.
- Kleinman, L. I., Daum, P. H., Lee, J. H., Lee, Y.-N., Nunnermacker, L. J., Springston, S. R., Newman, L., Weinstein-Lloyd, J., and Sillman, S.: Dependence of ozone production on NO and hydrocarbons in the troposphere, *Geophysical Research Letters*, 24, 2299–2302, doi:10.1029/97GL02279, 1997.
- 25 Krupa, S. V. and Manning, W. J.: Toxic Substance in the Environment Atmospheric ozone: Formation and effects on vegetation, *Environmental Pollution*, 50, 101–137, doi:10.1016/0269-7491(88)90187-X, <http://www.sciencedirect.com/science/article/pii/026974918890187X>, 1988.
- Kuhn, M., Builtjes, P. J. H., Poppe, D., Simpson, D., Stockwell, W. R., Andersson-Sköld, Y., Baart, A., Das, M., Fiedler, F., Hov, , Kirchner, F., Makar, P. A., Milford, J. B., Roemer, M. G. M., Ruhnke, R., Strand, A., Vogel, B., and Vogel, H.: Intercomparison of the gas-phase chemistry in several chemistry and transport models, *Atmospheric Environment*, 32, 693–709, doi:10.1016/S1352-2310(97)00329-4, <http://www.sciencedirect.com/science/article/pii/S1352231097003294>, 1998.
- 30

- Langridge, J. M., Gustafsson, R. J., Griffiths, P. T., Cox, R. A., Lambert, R. M., and Jones, R. L.: Solar driven nitrous acid formation on building material surfaces containing titanium dioxide: A concern for air quality in urban areas?, *Atmospheric Environment*, 43, 5128–5131, 2009.
- 35 Le Picard, S. D., Tizniti, M., Canosa, A., Sims, I. R., and Smith, I. W.: The thermodynamics of the elusive HO₃ radical, *Science*, 328, 1258–1262, 2010.
- Lee, J., Whalley, L., Heard, D., Stone, D., Dunmore, R., Hamilton, J., Young, D., Allan, J., Laufs, S., and Kleffmann, J.: Detailed budget analysis of HONO in central London reveals a missing daytime source, *Atmospheric Chemistry and Physics*, 16, 2747–2764, 2016.
- Li, G., Hu, J., Wang, S.-W., Georgopoulos, P. G., Schoendorf, J., and Rabitz, H.: Random Sampling-High Dimensional Model Representation (RS-HDMR) and Orthogonality of Its Different Order Component Functions, *J. Phys. Chem. A*, 110, 2474–2485, doi:10.1021/jp054148m, <http://dx.doi.org/10.1021/jp054148m>, 2006.
- Li, G., Rabitz, H., Yelvington, P. E., Oluwole, O. O., Bacon, F., Kolb, C. E., and Schoendorf, J.: Global Sensitivity Analysis for Systems with
5 Independent and/or Correlated Inputs, *J. Phys. Chem. A*, 114, 6022–6032, doi:10.1021/jp9096919, <http://dx.doi.org/10.1021/jp9096919>, 2010.
- Lu, K., Rohrer, F., Holland, F., Fuchs, H., Bohn, B., Brauers, T., Chang, C., Häsel, R., Hu, M., Kita, K., et al.: Observation and modelling of OH and HO₂ concentrations in the Pearl River Delta 2006: a missing OH source in a VOC rich atmosphere, *Atmospheric chemistry and physics*, 12, 1541–1569, 2012.
- 10 Lu, K., Hofzumahaus, A., Holland, F., Bohn, B., Brauers, T., Fuchs, H., Hu, M., Häsel, R., Kita, K., Kondo, Y., et al.: Missing OH source in a suburban environment near Beijing: observed and modelled OH and HO₂ concentrations in summer 2006, *Atmospheric Chemistry and Physics*, 13, 1057–1080, 2013.
- Luecken, D., Phillips, S., Sarwar, G., and Jang, C.: Effects of using the CB05 vs. SAPRC99 vs. CB4 chemical mechanism on model predictions: Ozone and gas-phase photochemical precursor concentrations, *Atmospheric Environment*, 42, 5805–5820, doi:10.1016/j.atmosenv.2007.08.056, <http://www.sciencedirect.com/science/article/pii/S1352231007007728>, 2008.
- 15 Luecken, D. J., Tonnesen, G. S., and Sickles, J. E., I.: Differences in NO_y speciation predicted by three photochemical mechanisms, *Atmospheric Environment*, 33, 1073–1084, doi:10.1016/S1352-2310(98)00319-7, <http://www.sciencedirect.com/science/article/pii/S1352231098003197>, 1999.
- Madronich, S. and Flocke, S.: The Role of Solar Radiation in Atmospheric Chemistry, in: *Environmental Photochemistry*, edited by Boule,
20 D. P., no. 2 / 2L in *The Handbook of Environmental Chemistry*, pp. 1–26, Springer Berlin Heidelberg, http://link.springer.com/chapter/10.1007/978-3-540-69044-3_1, 1999.
- Mao, J., Paulot, F., Jacob, D. J., Cohen, R. C., Crounse, J. D., Wennberg, P. O., Keller, C. A., Hudman, R. C., Barkley, M. P., and Horowitz, L. W.: Ozone and organic nitrates over the eastern United States: Sensitivity to isoprene chemistry, *Journal of Geophysical Research: Atmospheres*, 118, 2013.
- 25 Martinez, M., Harder, H., Kovacs, T. A., Simpas, J. B., Bassis, J., Leshner, R., Brune, W. H., Frost, G. J., Williams, E. J., Stroud, C. A., Jobson, B. T., Roberts, J. M., Hall, S. R., Shetter, R. E., Wert, B., Fried, A., Alicke, B., Stutz, J., Young, V. L., White, A. B., and Zamora, R. J.: OH and HO₂ concentrations, sources, and loss rates during the Southern Oxidants Study in Nashville, Tennessee, summer 1999, *Journal of Geophysical Research: Atmospheres*, 108, 4617–4634, doi:10.1029/2003JD003551, 2003.
- Mauldin, R. L., Cantrell, C. A., Zondlo, M., Kosciuch, E., Eisele, F. L., Chen, G., Davis, D., Weber, R., Crawford, J., Blake, D., Bandy, A.,
30 and Thornton, D.: Highlights of OH, H₂SO₄, and methane sulfonic acid measurements made aboard the NASA P-3B during Transport and Chemical Evolution over the Pacific : NASA global tropospheric experiment transport and chemical evolution over the Pacific (TRACE-

- P): Measurements and analysis (TRACEP1), *Journal of geophysical research*, 108, GTE17.1–GTE17.13, <http://cat.inist.fr/?aModele=afficheN&cpsidt=15353084>, 2003.
- 35 McDuffie, E. E., Edwards, P. M., Gilman, J. B., Lerner, B. M., Dubé, W. P., Trainer, M., Wolfe, D. E., Angevine, W. M., deGouw, J., Williams, E. J., et al.: Influence of oil and gas emissions on summertime ozone in the Colorado Northern Front Range, *Journal of Geophysical Research: Atmospheres*, 121, 8712–8729, 2016.
- Monge, M. E., D’Anna, B., Mazri, L., Giroir-Fendler, A., Ammann, M., Donaldson, D., and George, C.: Light changes the atmospheric reactivity of soot, *Proceedings of the National Academy of Sciences*, 107, 6605–6609, 2010.
- Müller, M., Mikoviny, T., Feil, S., Haidacher, S., Hanel, G., Hartungen, E., Jordan, A., Märk, L., Mutschlechner, P., Schottkowsky, R., Sulzer, P., Crawford, J. H., and Wisthaler, A.: A compact PTR-ToF-MS instrument for airborne measurements of volatile organic compounds at high spatiotemporal resolution, *Atmospheric Measurement Techniques*, 7, 3763–3772, doi:10.5194/amt-7-3763-2014, <http://www.atmos-meas-tech.net/7/3763/2014/>, 2014.
- 5 Murray, C., Derro, E. L., Sechler, T. D., and Lester, M. I.: Weakly bound molecules in the atmosphere: a case study of HOOO, *Accounts of chemical research*, 42, 419–427, 2008.
- Olson, J., Prather, M., Berntsen, T., Carmichael, G., Chatfield, R., Connell, P., Derwent, R., Horowitz, L., Jin, S., Kanakidou, M., Kasibhatla, P., Kotamarthi, R., Kuhn, M., Law, K., Penner, J., Perliski, L., Sillman, S., Stordal, F., Thompson, A., and Wild, O.: Results from the Intergovernmental Panel on Climatic Change Photochemical Model Intercomparison (PhotoComp), *J. Geophys. Res.*, 102, 5979–5991, doi:10.1029/96JD03380, <http://onlinelibrary.wiley.com/doi/10.1029/96JD03380/abstract>, 1997.
- Osthoff, H. D., Roberts, J. M., Ravishankara, A. R., Williams, E. J., Lerner, B. M., Sommariva, R., Bates, T. S., Coffman, D., Quinn, P. K., Dibb, J. E., Stark, H., Burkholder, J. B., Talukdar, R. K., Meagher, J., Fehsenfeld, F. C., and Brown, S. S.: High levels of nitryl chloride in the polluted subtropical marine boundary layer, *Nature Geosci*, 1, 324–328, doi:10.1038/ngeo177, <http://www.nature.com/ngeo/journal/v1/n5/full/ngeo177.html>, 2008.
- 15 Paulot, F., Crounse, J., Kjaergaard, H., Kroll, J., Seinfeld, J., and Wennberg, P.: Isoprene photooxidation: new insights into the production of acids and organic nitrates, *Atmospheric Chemistry and Physics*, 9, 1479–1501, 2009.
- Rabitz, H. and Alis, O. F.: General foundations of high-dimensional model representations, *Journal of Mathematical Chemistry*, 25, 197–233, doi:10.1023/A:1019188517934, <http://link.springer.com/article/10.1023/A%3A1019188517934>, 1999.
- 20 Ren, X., Harder, H., Martinez, M., Leshner, R. L., Oligier, A., Simpas, J. B., Brune, W. H., Schwab, J. J., Demerjian, K. L., He, Y., Zhou, X., and Gao, H.: OH and HO₂ Chemistry in the urban atmosphere of New York City, *Atmospheric Environment*, 37, 3639–3651, doi:10.1016/S1352-2310(03)00459-X, 2003.
- Ren, X., Brune, W. H., Cantrell, C. A., Edwards, G. D., Shirley, T., Metcalf, A. R., and Leshner, R. L.: Hydroxyl and Peroxy Radical Chemistry in a Rural Area of Central Pennsylvania: Observations and Model Comparisons, *J Atmos Chem*, 52, 231–257, doi:10.1007/s10874-005-3651-7, <http://link.springer.com/article/10.1007/s10874-005-3651-7>, 2005.
- 25 Ren, X., van Duin, D., Cazorla, M., Chen, S., Mao, J., Zhang, L., Brune, W. H., Flynn, J. H., Grossberg, N., Lefer, B. L., Rappenglück, B., Wong, K. W., Tsai, C., Stutz, J., Dibb, J. E., Thomas Jobson, B., Luke, W. T., and Kelley, P.: Atmospheric oxidation chemistry and ozone production: Results from SHARP 2009 in Houston, Texas, *Journal of Geophysical Research: Atmospheres*, 118, 5770–5780, doi:10.1002/jgrd.50342, 2013.
- 30 Riedel, T. P., Wagner, N. L., Dub, W. P., Middlebrook, A. M., Young, C. J., Öztürk, F., Bahreini, R., VandenBoer, T. C., Wolfe, D. E., Williams, E. J., Roberts, J. M., Brown, S. S., and Thornton, J. A.: Chlorine activation within urban or power plant plumes: Vertically

- resolved ClNO₂ and Cl₂ measurements from a tall tower in a polluted continental setting, *J. Geophys. Res. Atmos.*, 118, 8702–8715, doi:10.1002/jgrd.50637, <http://onlinelibrary.wiley.com/doi/10.1002/jgrd.50637/abstract>, 2013.
- Riedel, T. P., Wolfe, G. M., Danas, K. T., Gilman, J. B., Kuster, W. C., Bon, D. M., Vlasenko, A., Li, S.-M., Williams, E. J., Lerner, B. M., Veres, P. R., Roberts, J. M., Holloway, J. S., Lefer, B., Brown, S. S., and Thornton, J. A.: An MCM modeling study of nitryl chloride (ClNO₂) impacts on oxidation, ozone production and nitrogen oxide partitioning in polluted continental outflow, *Atmos. Chem. Phys.*, 14, 3789–3800, doi:10.5194/acp-14-3789-2014, <http://www.atmos-chem-phys.net/14/3789/2014/>, 2014.
- Roberts, J. M., Osthoff, H. D., Brown, S. S., Ravishankara, A. R., Coffman, D., Quinn, P., and Bates, T.: Laboratory studies of products of N₂O₅ uptake on Cl₂ containing substrates, *Geophys. Res. Lett.*, 36, L20 808, doi:10.1029/2009GL040448, <http://onlinelibrary.wiley.com/doi/10.1029/2009GL040448/abstract>, 2009.
- Rohrer, F., Bohn, B., Brauers, T., Brüning, D., Johnen, F.-J., Wahner, A., and Kleffmann, J.: Characterisation of the photolytic HONO-source in the atmosphere simulation chamber SAPHIR, *Atmos. Chem. Phys.*, 5, 2189–2201, doi:10.5194/acp-5-2189-2005, 2005.
- Rolph, G.: READY - Real-time Environmental Applications and Display sYstem, <http://ready.arl.noaa.gov>: Accessed 3 Jan. 2016., 2016.
- Sander, S., Abbatt, J., Barker, J., Burkholder, J., Friedl, R., Golden, D., Huie, R., Kolb, C., Kurylo, M., Moortgat, G., Orkin, V., and Wine, P.: Chemical Kinetics and Photochemical Data for Use in Atmospheric Studies, Evaluation No. 17, JPL Publication 10-6, <http://jpldataeval.jpl.nasa.gov>, 2011.
- Saunders, S. M., Jenkin, M. E., Derwent, R. G., and Pilling, M. J.: Protocol for the development of the Master Chemical Mechanism, MCM v3 (Part A): tropospheric degradation of non-aromatic volatile organic compounds, *Atmospheric Chemistry and Physics*, 3, 161–180, doi:10.5194/acp-3-161-2003, <http://www.atmos-chem-phys.net/3/161/2003/>, 2003.
- Seinfeld, J. H. and Pandis, S. N.: Atmospheric chemistry and physics: from air pollution to climate change, John Wiley & Sons, 2012.
- Sheehy, P., Volkamer, R., Molina, L., and Molina, M.: Oxidative capacity of the Mexico City atmosphere–Part 2: A RO_x radical cycling perspective, *Atmospheric Chemistry and Physics*, 10, 6993–7008, 2010.
- Shirley, T., Brune, W., Ren, X., Mao, J., Leshner, R., Cardenas, B., Volkamer, R., Molina, L., Molina, M. J., Lamb, B., et al.: Atmospheric oxidation in the Mexico City metropolitan area (MCMA) during April 2003, *Atmospheric Chemistry and Physics*, 6, 2753–2765, 2006.
- Spencer, K., McCabe, D., Crounse, J., Olson, J., Crawford, J., Weinheimer, A., Knapp, D., Montzka, D., Cantrell, C., Hornbrook, R., et al.: Inferring ozone production in an urban atmosphere using measurements of peroxyacetic acid, *Atmospheric Chemistry and Physics*, 9, 3697–3707, 2009.
- Stein, A. F., Draxler, R. R., Rolph, G. D., Stunder, B. J. B., Cohen, M. D., and Ngan, F.: NOAA’s HYSPLIT Atmospheric Transport and Dispersion Modeling System, *Bull. Amer. Meteor. Soc.*, 96, 2059–2077, doi:10.1175/BAMS-D-14-00110.1, <http://journals.ametsoc.org/doi/10.1175/BAMS-D-14-00110.1>, 2015.
- Stemmler, K., Ammann, M., Donders, C., Kleffmann, J., and George, C.: Photosensitized reduction of nitrogen dioxide on humic acid as a source of nitrous acid, *Nature*, 440, 195–198, 2006.
- Stockwell, W. R., Kirchner, F., Kuhn, M., and Seefeld, S.: A new mechanism for regional atmospheric chemistry modeling, *Journal of Geophysical Research: Atmospheres*, 102, 25 847 – 25 879, doi:10.1029/97JD00849, 1997.
- Stone, D., Whalley, L. K., and Heard, D. E.: Tropospheric OH and HO₂ radicals: field measurements and model comparisons, *Chem. Soc. Rev.*, 41, 6348–6404, doi:10.1039/C2CS35140D, <http://dx.doi.org/10.1039/C2CS35140D>, 2012.
- Tan, Z., Fuchs, H., Lu, K., Hofzumahaus, A., Bohn, B., Broch, S., Dong, H., Gomm, S., Häsel, R., He, L., Holland, F., Li, X., Liu, Y., Lu, S., Rohrer, F., Shao, M., Wang, B., Wang, M., Wu, Y., Zeng, L., Zhang, Y., Wahner, A., and Zhang, Y.: Radical chemistry at a rural

- site (Wangdu) in the North China Plain: observation and model calculations of OH, HO₂ and RO₂ radicals, *Atmospheric Chemistry and Physics*, 17, 663–690, doi:10.5194/acp-17-663-2017, <http://www.atmos-chem-phys.net/17/663/2017/>, 2017.
- 35 Thornton, J. A. and Abbatt, J. P. D.: N₂O₅ Reaction on Submicron Sea Salt Aerosol: Kinetics, Products, and the Effect of Surface Active Organics, *J. Phys. Chem. A*, 109, 10 004–10 012, doi:10.1021/jp054183t, <http://dx.doi.org/10.1021/jp054183t>, 2005.
- Thornton, J. A., Wooldridge, P. J., Cohen, R. C., Martinez, M., Harder, H., Brune, W. H., Williams, E. J., Roberts, J. M., Fehsenfeld, F. C., Hall, S. R., Shetter, R. E., Wert, B. P., and Fried, A.: Ozone production rates as a function of NO_x abundances and HO_x production rates in the Nashville urban plume, *Journal of Geophysical Research: Atmospheres*, 107, 7–17, doi:10.1029/2001JD000932, 2002.
- Thornton, J. A., Kercher, J. P., Riedel, T. P., Wagner, N. L., Cozic, J., Holloway, J. S., Dubé, W. P., Wolfe, G. M., Quinn, P. K., Middlebrook, A. M., Alexander, B., and Brown, S. S.: A large atomic chlorine source inferred from mid-continental reactive nitrogen chemistry, *Nature*, 464, 271–274, doi:10.1038/nature08905, <http://www.nature.com/nature/journal/v464/n7286/full/nature08905.html>, 2010.
- 5 Tonnesen, G. S. and Dennis, R. L.: Analysis of radical propagation efficiency to assess ozone sensitivity to hydrocarbons and NO_x : 1. Local indicators of instantaneous odd oxygen production sensitivity, *Journal of Geophysical Research: Atmospheres*, 105, 9213–9225, doi:10.1029/1999JD900371, 2000.
- Trainer, M., Parrish, D. D., Goldan, P. D., Roberts, J., and Fehsenfeld, F. C.: Review of observation-based analysis of the regional factors influencing ozone concentrations, *Atmospheric Environment*, 34, 2045–2061, doi:10.1016/S1352-2310(99)00459-8, <http://www.sciencedirect.com/science/article/pii/S1352231099004598>, 2000.
- 10 Treadaway, V.: Measurement of Formic and Acetic Acid in Air by Chemical Ionization Mass Spectroscopy: Airborne Method Development, Master's thesis, University of Rhode Island, <http://digitalcommons.uri.edu/theses/603>, Paper 603, 2015.
- Trebs, I., Bohn, B., Ammann, C., Rummel, U., Blumthaler, M., Königstedt, R., Meixner, F. X., Fan, S., and Andreae, M. O.: Relationship between the NO₂ photolysis frequency and the solar global irradiance, *Atmospheric Measurement Techniques*, 2, 725–739, doi:10.5194/amt-2-725-2009, <http://www.atmos-meas-tech.net/2/725/2009/>, 2009.
- 15 US EPA: Laboratory study to explore potential interferences to air quality monitors, Govt. Doc. EP 4.52:2002006990, Office of Air Quality Planning and Standards, Research Triangle Park, NC Accessed online: 2014-01-04, 1999.
- US EPA: Integrated Science Assessment of Ozone and Related Photochemical Oxidants(Final Report), Govt. Doc. EPA/600/R - 10/076F, Office of Research and Development, National Center for Environmental Assessment- RTP Division, Research Triangle Park, NC, 2013.
- US EPA: Ozone Trends, <https://www.epa.gov/air-trends/ozone-trends>, Accessed 22 April 2016., 2016a.
- 20 US EPA: Ozone NAAQS | US EPA, https://www3.epa.gov/ttn/naaqs/standards/ozone/s_o3_index.html, 2016b.
- VandenBoer, T. C., Brown, S. S., Murphy, J. G., Keene, W. C., Young, C. J., Pszenny, A., Kim, S., Warneke, C., Gouw, J. A., Maben, J. R., et al.: Understanding the role of the ground surface in HONO vertical structure: High resolution vertical profiles during NACHTT-11, *Journal of Geophysical Research: Atmospheres*, 118, 2013.
- VandenBoer, T. C., Young, C. J., Talukdar, R. K., Markovic, M. Z., Brown, S. S., Roberts, J. M., and Murphy, J. G.: Nocturnal loss and daytime source of nitrous acid through reactive uptake and displacement, *Nature Geoscience*, 8, 55–60, 2015.
- 25 Volkamer, R., Sheehy, P., Molina, L., and Molina, M.: Oxidative capacity of the Mexico City atmosphere—Part I: A radical source perspective, *Atmospheric Chemistry and Physics*, 10, 6969–6991, 2010.
- Wagner, N. L., Riedel, T. P., Young, C. J., Bahreini, R., Brock, C. A., Dubé, W. P., Kim, S., Middlebrook, A. M., Öztürk, F., Roberts, J. M., Russo, R., Sive, B., Swarthout, R., Thornton, J. A., VandenBoer, T. C., Zhou, Y., and Brown, S. S.: N₂O₅ uptake coefficients and nocturnal NO₂ removal rates determined from ambient wintertime measurements, *J. Geophys. Res. Atmos.*, 118, 9331–9350, doi:10.1002/jgrd.50653, <http://onlinelibrary.wiley.com/doi/10.1002/jgrd.50653/abstract>, 2013.

- Wainman, T., Weschler, C. J., Lioy, P. J., and Zhang, J.: Effects of surface type and relative humidity on the production and concentration of nitrous acid in a model indoor environment, *Environmental Science & Technology*, 35, 2201–2206, PMID: 11414019, 2001.
- 1025 Weibring, P., Richter, D., Fried, A., Walega, J., and Dyroff, C.: Ultra-high-precision mid-IR spectrometer II: system description and spectroscopic performance, *Applied Physics B*, 85, 207–218, 2006.
- Weibring, P., Richter, D., Walega, J. G., and Fried, A.: First demonstration of a high performance difference frequency spectrometer on airborne platforms, *Optics Express*, 15, 13 476–13 495, 2007.
- Wilson, K. L. and Birks, J. W.: Mechanism and elimination of a water vapor interference in the measurement of ozone by UV absorbance, *Environmental Science & Technology*, 40, 6361–6367, PMID: 17120566, 2006.
- 1030 Wolfe, G. M., Thornton, J. A., Bouvier-Brown, N. C., Goldstein, A. H., Park, J.-H., McKay, M., Matross, D. M., Mao, J., Brune, W. H., LaFranchi, B. W., Browne, E. C., Min, K.-E., Wooldridge, P. J., Cohen, R. C., Crouse, J. D., Faloona, I. C., Gilman, J. B., Kuster, W. C., de Gouw, J. A., Huisman, A., and Keutsch, F. N.: The Chemistry of Atmosphere-Forest Exchange (CAFE) Model Part 2: Application to BEARPEX-2007 observations, *Atmos. Chem. Phys.*, 11, 1269–1294, doi:10.5194/acp-11-1269-2011, <http://www.atmos-chem-phys.net/11/1269/2011/>, 2011.
- 1035 Wolfe, G. M., Marvin, M. R., Roberts, S. J., Travis, K. R., and Liao, J.: The Framework for 0-D Atmospheric Modeling (F0AM) v3.1, *Geoscientific Model Development*, 9, 3309–3319, doi:10.5194/gmd-9-3309-2016, <http://www.geosci-model-dev.net/9/3309/2016/>, 2016.
- Xue, L. K., Saunders, S. M., Wang, T., Gao, R., Wang, X. F., Zhang, Q. Z., and Wang, W. X.: Development of a chlorine chemistry module for the Master Chemical Mechanism, *Geosci. Model Dev.*, 8, 3151–3162, doi:10.5194/gmd-8-3151-2015, <http://www.geosci-model-dev.net/8/3151/2015/>, 2015.
- 1040 Zetzsch, C. and Behnke, W.: Heterogeneous Photochemical Sources of Atomic Cl in the Troposphere, *Berichte der Bunsengesellschaft physikalische Chemie*, 96, 488–493, doi:10.1002/bbpc.19920960351, <http://onlinelibrary.wiley.com/doi/10.1002/bbpc.19920960351/abstract>, 1992.
- Zheng, W., Flocke, F. M., Tyndall, G. S., Swanson, A., Orlando, J. J., Roberts, J. M., Huey, L. G., and Tanner, D. J.: Characterization of a thermal decomposition chemical ionization mass spectrometer for the measurement of peroxy acyl nitrates (PANs) in the atmosphere, *Atmospheric Chemistry and Physics*, 11, 6529–6547, doi:10.5194/acp-11-6529-2011, <http://www.atmos-chem-phys.net/11/6529/2011/>, 2011.
- 1045 Zhou, X., Gao, H., He, Y., Huang, G., Bertman, S. B., Civerolo, K., and Schwab, J.: Nitric acid photolysis on surfaces in low-NO_x environments: Significant atmospheric implications, *Geophysical Research Letters*, 30, 2217—2221, doi:10.1029/2003GL018620, 2003.
- 1050 Zhou, X., Zhang, N., TerAvest, M., Tang, D., Hou, J., Bertman, S., Alaghmand, M., Shepson, P. B., Carroll, M. A., Griffith, S., et al.: Nitric acid photolysis on forest canopy surface as a source for tropospheric nitrous acid, *Nature Geoscience*, 4, 440–443, 2011.

Table 1. Measured parameters input into the RACM2 and MCMv331. Inorganic chemical species measurement time resolution is 1 min. Aircraft chemical species were measured every 1 s. Evacuated whole-air canister VOC point measurements were interpolated to 1-h medians as described in Section 2.2. All measured constraints were either averaged or interpolated to 10 min for model runs.

Number	Model input	Method ^b	Uncertainty (%)	Institution
8	Inorganics O ₃ SO ₂ NO ₂ , NO CO, CO ₂ , CH ₄ HNO ₃	CL UV Fluorescence CES/CAPS, CL WACs/GC/GC-MS (Colman et al., 2001) TD-LIF (Day et al., 2002)	10 10 10 ≤ 5 25	EPA UCI UC Berkeley ^a
58	Organic Species			
42	<i>C</i> ₂ - <i>C</i> ₁₀ <i>NMHCs</i> , <i>organic nitrates</i> : ethane, ethene, acetylene, propane, propene, i-butane, n-butane, i-pentane, n-pentane, isoprene, n-hexane, n-heptane, n-octane, 2,3-dimethylbutane, 2-methylpentane, 3-methylpentane, 2,4-dimethylpentane, 2,2,4-trimethylpentane, cyclopentane, methylcyclopentane, cyclohexane, methylcyclohexane, benzene, toluene, ethylbenzene, m,p-xylene, o-xylene, 2-ethyltoluene, 3-ethyltoluene, 4-ethyltoluene, 1,3,5-trimethylbenzene, 1,2,4-trimethylbenzene, 1,2,3-trimethylbenzene, α -pinene, β -pinene, methyl nitrate, ethyl nitrate, i-propylnitrate, 2-butylnitrate, 2-pentylnitrate, 3-pentylnitrate, 2-methyl-2-butylnitrate	WACs/GC/GC-MS (Colman et al., 2001)	3-100	UCI
	<i>NMHCs</i> ^a : methyl ethyl ketone, methanol, methyl vinyl ketone, methacrolein, acetic acid acetaldehyde, acetone formaldehyde	PTR-ToF-MS (Müller et al., 2014)	10	U. Innsbruck
	<i>peroxy-peroxy</i> acetyl nitrate, <i>peroxy-peroxy</i> propyl nitrate	DFGAS (Weibring et al., 2006, 2007) PAN-CIMS (Zheng et al., 2011)	5 13	CU-INSTAAR NCAR
	hydrogen peroxide, formic acid, acetic acid	PCIMS (Treadaway, 2015)	30	URI
	ethanol, d-limonene/3-carene, camphene	TOGA (Apel et al., 2003)	30	NCAR

^a Denotes aircraft measurements

^b CL, chemiluminescence; CES, cavity enhanced spectroscopy; CAPS, cavity attenuated phase shift spectrometer; WAC, whole-air canister; GC, gas chromatography; GC-MS, gas chromatography mass spectrometer; TD-LIF, thermal dissociation laser-induced fluorescence; PTR-ToF-MS, proton transfer reaction time-of-flight mass spectrometer; DFGAS, difference frequency generation absorption spectrometer; CIMS, chemical ionization mass spectrometer ('PAN', peroxyacyl nitrate; 'P', peroxide); TOGA, trace organic gas analyzer.

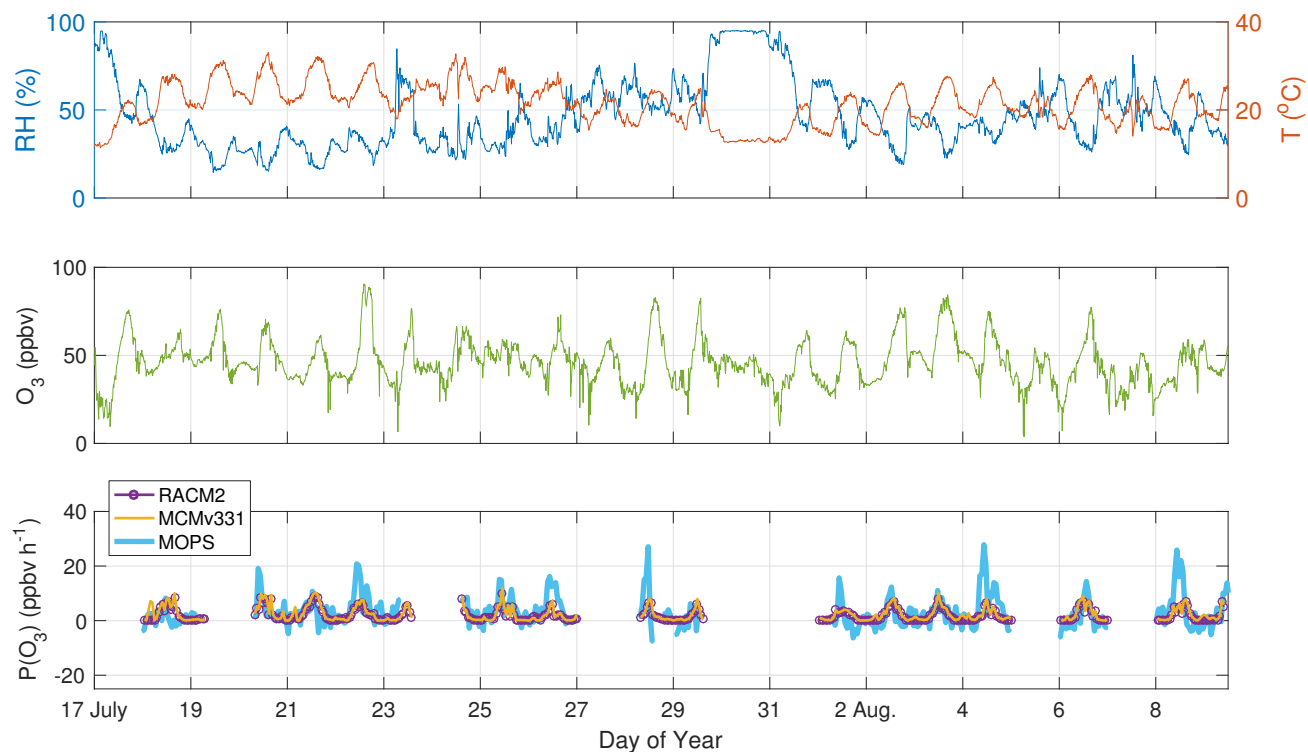


Figure 1. Top: Full-campaign 10-minute temperature and relative humidity in Golden, CO. The “warm” period is defined as days before 27 July 2014. Middle: Full-campaign 10-min O_3 mixing ratios for 17 July to 10 August 2014. Bottom: $P(O_3)$ measured by the MOPS and modeled from the RACM2 and MCMv331 for the same time period. Measured to modeled comparisons are shown for days with available MOPS measurements and have are averaged over a 30-min-1-hour time resolution period.

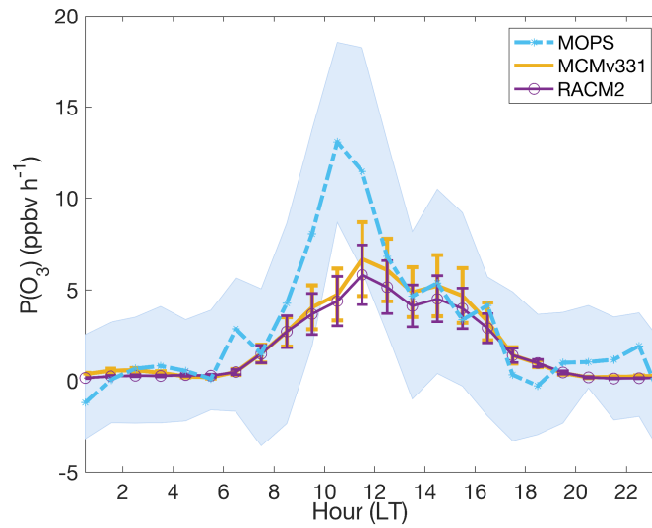
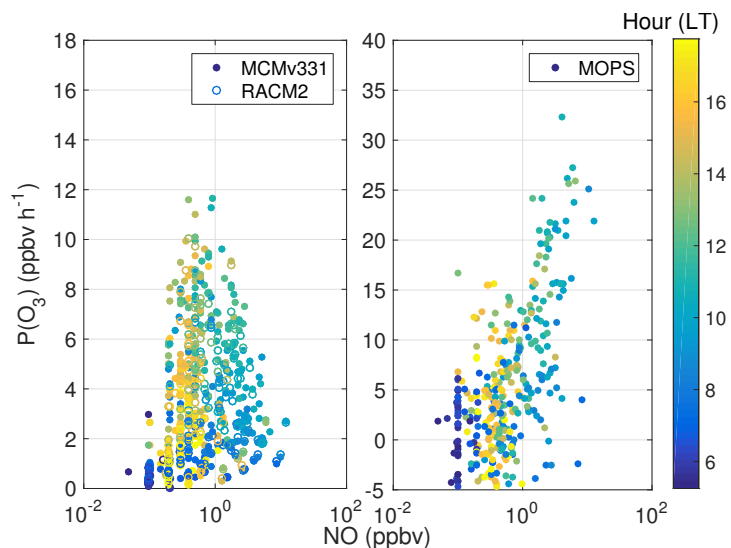


Figure 2. Full-campaign median hourly $P(O_3)$ measured by the MOPS, and modeled by the RACM2 and MCMv331 for daylight hours between 0600–1800 local time. Diel values shown are shown only for days with MOPS measurements measurement days. The Shaded areas represent the variance in MOPS absolute standard deviation $P(1\sigma O_3)$ is shown for 1600 and due to the variation in the zero correction. The RACM2 and MCMv331 relative error bars are shown at the 1σ confidence level. Shown as a shaded area is the MOPS 25th and 75th percentiles.



RACM2, MCMv331 (left), and MOPS (right) 30-minute $P(O_3)$ as a function NO for total campaign data all MOPS measurement days. Points are colored by hour of day from 0600-1800 LT.

RACM2, MCMv331 (left), and MOPS (right) 30-minute $P(O_3)$ as a function NO for total campaign data all MOPS measurement days. Points are colored by hour of day from 0600-1800 LT.

Figure 3. C-130 aircraft CIMS HO_2/OH ratio as a function of aircraft NO (chemiluminescence, 20 pptv \pm 10%, 1σ uncertainty) around the vicinity of Golden, CO, and modeled HO_2/OH ratio using constrained NO measured in Golden, CO. Aircraft measurements used are limited to the first 1 km in the boundary layer, and a well-mixed boundary layer is assumed for the HO_x measurements. MCMv331 model results are shown for the $OH + NO + O_2$ reaction to yield $HO_2 + NO_2$ using the kinetic rate coefficient of $(9-15) \times 10^{-11} \text{ cm}^3 \text{ molecule}^{-1} \text{ s}^{-1}$ discussed in Section ??.

RACM2, MCMv331 (left), and MOPS (right) 30-minute $P(O_3)$ as a function NO for total campaign data all MOPS measurement days. Points are colored by hour of day from 0600-1800 LT.

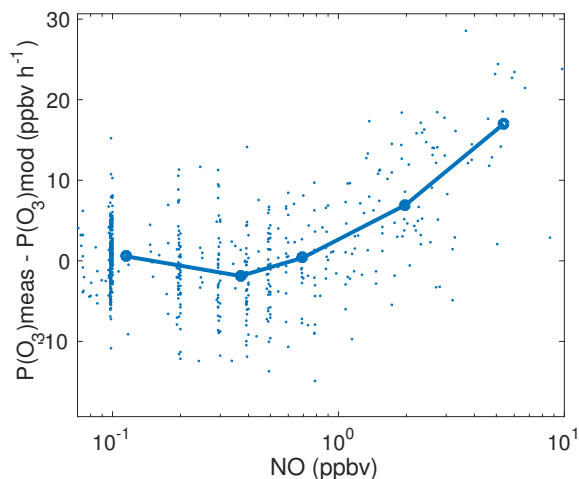


Figure 4. Difference between $P(O_3)$ measured and modeled as a function of measured NO. Individual points are averaged for 30 minutes, while the solid line indicates the average $P(O_3)$ difference binned by NO.

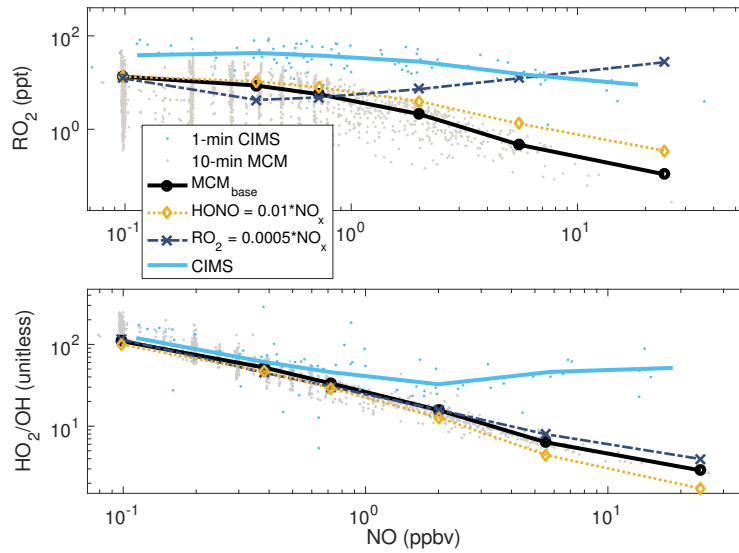


Figure 5. C-130 CIMS HO_2/OH ratio and RO_2 as a function of aircraft NO (chemiluminescence, $20 \text{ pptv} \pm 10\%$, 1σ uncertainty) and modeled HO_2/OH ratio and RO_2 versus constrained NO measured continuously in Golden, CO. Aircraft measurements used are limited to the first 1 km in the boundary layer and for only times when the C-130 was within 20 km of Golden, CO. A well-mixed boundary layer is assumed for all measurements.

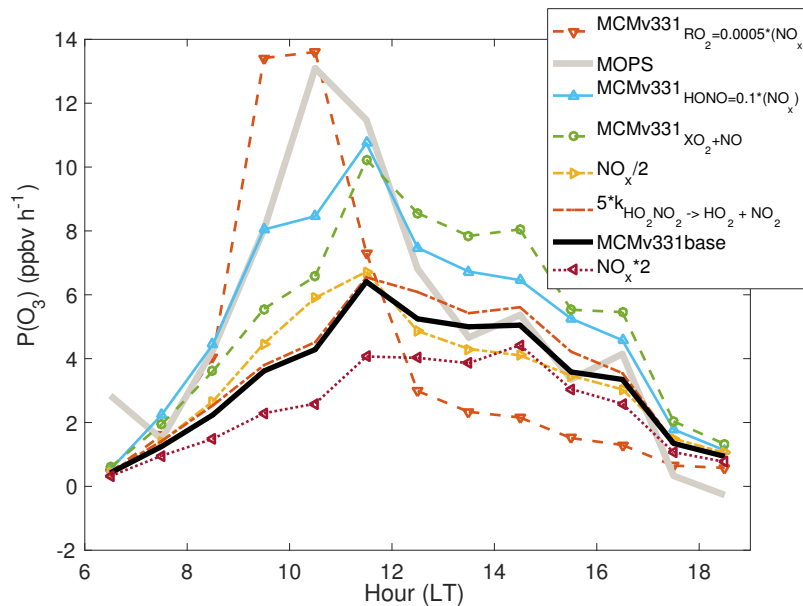


Figure 6. Model $\text{P}(\text{O}_3)$ scenarios using MCMv331 calculated for daytime $\text{P}(\text{O}_3)$ hours between 0600 and 1800 LT. Median hourly $\text{P}(\text{O}_3)$ is derived from the model case studies described in the main text and compared to the MOPs median diel $\text{P}(\text{O}_3)$ and MCMv331 median diel base case.

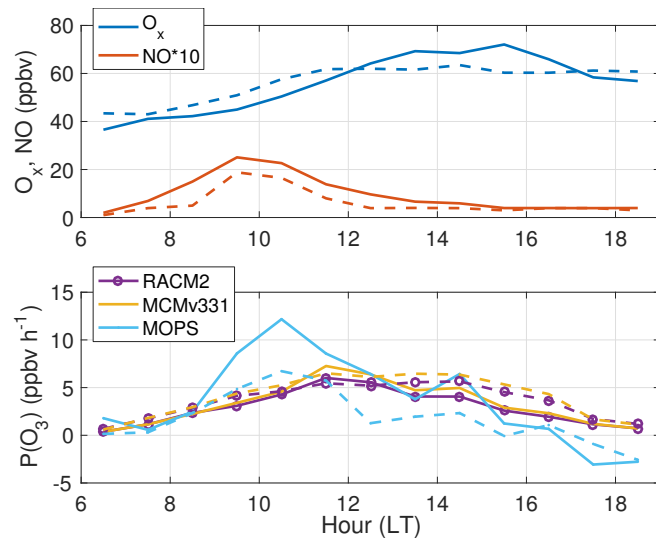


Figure 7. Top: O_x (O₃ + NO₂) and NO mixing ratios for Denver plume (solid) versus all other days (dashed) from 17 July - 10 August 2014 in Golden, CO. Bottom: Median measured and modeled P(O₃) for Denver plume (solid) and non-Denver plume (dashed) days between 0600-1800 LT.